

Brane Stabilization and *Regionality* of Extra Dimensions

David M. Jacobs*, Glenn D. Starkman†, and Andrew J. Tolley‡

Center for Education and Research in Cosmology and Astrophysics and

Department of Physics and Institute for the Science of Origins,

Case Western Reserve University

Extra dimensions are a common feature of beyond the Standard Model physics. In a braneworld scenario, local physics on the brane can depend strongly on the brane's location within the bulk. Generically, the relevant properties of the bulk manifold for the physics on/of the brane are neither local nor global, but depend on the structure of finite regions of the bulk, even for locally homogeneous and isotropic bulk geometries. In a recent work we considered various mechanisms (in a braneworld context) to stabilize the location of a brane within bulk spaces of non-trivial topology. In this work we elaborate on and generalize that work by considering additional bulk and brane dimensionalities as well as different boundary conditions on the bulk scalar field that provides a Casimir force on the brane, providing further insight on this effect.

In $D = 2 + 1$ ($D = 5 + 1$) we consider both local and global contributions to the effective potential of a 1-brane (4-brane) wrapped around both the 2-dimensional hyperbolic horn and Euclidean cone, which are used as toy models of an extra-dimensional manifold. We calculate the total energy due to brane tension and elastic energy (extrinsic curvature) as well as that due to the Casimir energy of a bulk scalar satisfying both Dirichlet and Neumann boundary conditions on the brane. In some cases stable minima of the potential are found that result from the competition of at least two of the contributions. Generically, any one of these effects may be sufficient when the bulk space has less symmetry than the manifolds considered here. We highlight the importance of the Casimir effect for the purpose of brane stabilization.

* Email address: david.m.jacobs@case.edu

† Email address: glenn.starkman@case.edu

‡ Email address: andrew.j.tolley@case.edu

Contents

I. Introduction	3
II. Hyperbolic Horn	8
A. Preliminaries	8
1. The Model, Energy Contributions, and Bulk ϕ Solutions	8
2. Procedure for Calculation of Casimir Energy on the Horn	12
B. $D = 2 + 1$	15
1. Dirichlet Condition	15
2. Neumann Condition	17
C. $D = 5 + 1$	17
1. Dirichlet Condition	19
2. Neumann Condition	21
III. Euclidean Cone	22
A. Preliminaries	22
1. The Model, Energy Contributions, and Bulk ϕ Solutions	22
2. Procedure for Calculation of Casimir Energy on the Cone	25
B. $D = 2 + 1$	27
1. Dirichlet Condition	27
2. Neumann Condition	29
C. $D = 5 + 1$	30
1. Dirichlet Condition	31
2. Neumann Condition	33
IV. Conclusions	33
References	36
A. Details of Mode Solutions	38
1. Hyperbolic Horn	38
a. $n \neq 0$	38
b. $n = 0$	39

2. Euclidean Cone	40
B. Calculating $E_0(s)$ via Contour Integrals	40
1. General Procedure	40
2. Horn Generating Functions (Dirichlet, $n \neq 0$)	41
3. Horn Generating Functions (Dirichlet, $n = 0$)	42
4. Cone Generating Functions	43
C. Bessel Function Asymptotics	44
D. Details of $2 + 1$ Horn Calculation	45
1. $E_0^{\text{div}}(s)$	45
2. E_0^{rem}	46
3. E_0^{fin}	46
E. Heat Kernel Analysis	48
1. Heat Kernel Analysis of a General $E_0(s)$	48
2. Heat Kernel Technique Applied to the $D = 2 + 1$ Geometries	49
a. Hyperbolic Horn	49
b. Euclidean Cone	50

I. INTRODUCTION

Several outstanding problems remain in fundamental physics. To name a few: unification of the gauge interactions of the Standard Model with the gravitational interaction, the enormous hierarchy between the observed gravitational and weak scales, $M_{\text{pl}}/M_{\text{weak}} \approx 10^{17}$, as well as the hierarchy among fundamental fermion masses (e.g. $m_\tau/m_e \approx 3500$), and the smallness of an apparent cosmological constant, Λ , where $\sqrt{\Lambda} \approx H_0 \approx 10^{-33} \text{eV} \approx 10^{-44} M_{\text{weak}}^{[1]}$.

Extra spatial dimensions might exist and may help to explain some, if not all of these issues: they are an essential feature of string theory; “large” extra dimensions have been employed in attempts to explain the weak (e.g. [1–3]) and flavor (e.g. [4]) hierarchies; there

[1] As usual we have set $\hbar = c = 1$.

have also been attempts to address the dark energy problem via infra-red modifications of gravity that employ extra dimensions (e.g. [5–7]).

Common experience and laboratory experiments tell us we don’t appear to live in more than three spatial dimensions; if more exist they should be hidden in some way. One explanation might be that the Standard Model fields are confined to submanifolds of lower dimension or perhaps the extra dimensions are compactified (i.e. the manifold has non-trivial topology) to length scales that have remained inaccessible by experiments. The actual situation may be a combination of both. Furthermore, since topology is a *global* property of the space-time manifold it cannot be determined by the *local* Einstein’s equations – interestingly, though, topology can have a large influence on local physical processes within the manifold.

In what follows below we will consider scenarios where the full space-time manifold is the direct product of 4D Minkowski space-time, \mathcal{M}^4 , (or similarly, Friedmann-Robertson-Walker) with a d -dimensional extra manifold, Ω^d , but certainly the discussion could extend to other scenarios. With $d = 1$ only the topology needs to be specified, as the geometry is trivial. From experience we know geometry can play an important role as well, therefore we begin our discussion with $d = 2$.

Let us first consider a cylinder with topology $(\mathbb{R} \times S^1)$. It can be obtained from Euclidean 2-space (E^2) by modding out by a group (Γ) of 1-dimensional discrete translations. The local geometry remains the same as the covering space (i.e. homogeneous and isotropic), however the presence of fields indicates that some (global) symmetry has been broken. For example, the components of field momenta are quantized in the compact dimension, while they remain continuous in the infinite dimension. That is, local experiments are sensitive to the global structure of the manifold. Even so, *no special places exist on this space*, as the results of such experiments are insensitive to where on the manifold they are performed.

This should be contrasted with the two-dimensional hyperbolic horn (\mathcal{H}^2/Γ), obtained from the hyperbolic 2-space \mathcal{H}^2 by modding out by the same Γ (see Figure 1). Fields on this space indicate that both rotational *and* translational symmetry are broken; field modes with non-zero excitation in the compact dimension are highly inhomogeneous in z and are doubly exponentially suppressed beyond the point on the manifold where the “circumference” of the compact dimension becomes smaller than the mode wavelength. In other words, modes of a certain momentum can only be sent a finite distance down the horn. Since translation

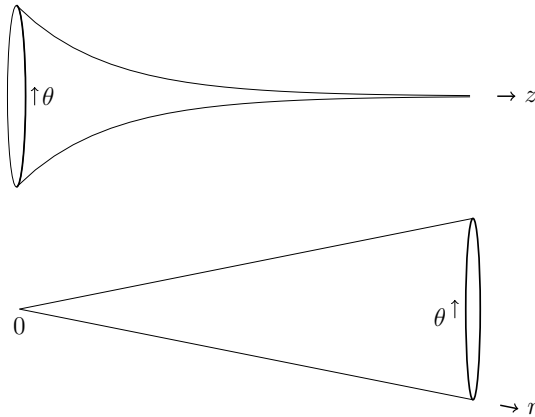


FIG. 1: Horn (top) and Cone (bottom) topologies.

invariance is broken, there exists a notion of absolute position and the results of local experiments will vary along the length of the horn. The main lesson here is that even if the local geometry of a manifold is homogeneous and isotropic, the physics on it will generally not be.

The physically relevant scale in this example is the horn circumference, a quantity that is sensitive to non-local characteristics of the manifold, yet is insensitive to whether or not the manifold is actually entirely a horn that extends to infinity with infinite volume. For this reason we term such a quantity *regional*, a quantity that could not have been calculated simply using local geometric information, yet did not require complete knowledge of the manifold’s structure. The hyperbolic horn is of great utility because it has a lot of the salient features of more generic manifolds, in particular the “cuspy” regions of compact hyperbolic manifolds (CHMs)^[2]. It therefore seems that what may appear as a global effect can actually be attributed to the regional structure of the manifold one considers.

Another simple but non-trivial topology is that of a cone, a two-dimensional Euclidean space with a “wedge” removed from it. It is obtained by identifying $\theta \leftrightarrow \theta + 2\pi(1 - \delta)$, when working in polar coordinates, r and θ (see Figure 1). Topologically, the space is given by $\mathbb{R}^2 - \{0\}$, i.e. the point at the tip of the cone is removed from the manifold. Again,

[2] CHMs provide an appealing geometric solution for the hierarchy problem (see [8]); they could be considered a hyperbolic, $d > 1$, version of models discussed in [1] or [3], wherein all but one modulus is fixed. CHM’s have also found use in string theory (see e.g. [9]).

translation invariance is broken, as the distance from the tip of the cone is imprinted on the modes. The cone offers a complementary example to the horn as it has zero curvature and is a better approximation to regions of manifolds that are geometrically flat and end in a vertex.

We would like to focus our attention on braneworld scenarios and the local physical consequences of regional properties of the bulk manifold. They would affect, e.g. vacuum energy of a brane itself, as it is generically proportional to the inverse of the brane volume, which can vary as the brane is moved through the manifold. Furthermore, the amplitude for brane fields to interact with fields in the bulk (e.g. the gravitational field) would also be sensitive to the position of the brane, as the structure of bulk modes are generally inhomogeneous. Finally, as we shall explore in this work, there are local forces on branes arising from e.g. the Casimir effect of bulk fields interacting with the brane.

Before exploring any interesting phenomenological prospects, however, we must ask what determines the brane's location within the bulk and what ensures it is stabilized. From an effective 4D perspective the brane's position within the bulk appears as a series of massless scalar fields, one for each of the brane's codimensions. Observational constraints on fifth forces tell us that such fields should have a mass $\gtrsim 10^{-3}$ eV [10] if they couple to matter with gravitational strength. In any case, stability is a reasonable requirement of any system and thus the brane's effective potential should have a stable minimum in which it sits. Stabilizing a brane in this context should be contrasted with other mechanisms (e.g. [11]) that have been used in the context of stabilizing the moduli of the bulk – here we are concerned with determining and stabilizing the brane position *within* a bulk that is assumed to be stable.

In this work we focus on different local (geometric) and global contributions to the brane potential and find that they depend on the manifold's non-trivial structure in different ways. From classical intuition, we expect that a brane's non-zero tension will provide an energy proportional to the brane volume. Furthermore, there will generally be an elastic energy associated with the brane's extrinsic curvature and how it couples to the intrinsic bulk curvature.

Due to local interactions with the brane, inhomogeneities in bulk field modes will be induced – this will be approximated here by an effective boundary condition on the bulk field(s) at the location of the brane. Therefore if global translation invariance of the bulk manifold is broken, the vacuum energy of bulk fields (a global quantity) will depend on

the location of the brane, providing a location-dependent force, i.e. the Casimir effect [12]. Likewise, the Casimir energy of Standard Model fields living on the brane can play a role if the brane’s topology is non-trivial. Calculation of Casimir energies is subtle because it strongly depends on the bulk and boundary geometry, topology, dimensionality, field type, and boundary conditions. The magnitude of the effect can be estimated on dimensional grounds; however in order to get the overall sign and precise magnitude of the energy, a full calculation usually must be performed. Having explicit analytic expressions for the fields modes (as one has on the horn and cone) makes this task much more tractable.

Though using Casimir energies to stabilize bulk moduli is not a new idea (see e.g [13–16]), to our knowledge they have not been used to stabilize the location of a single brane within the bulk nor have the regional properties of manifolds been exploited for their use. We would especially like to emphasize the role of the Casimir effect because, in the case of a 3-brane embedded in a higher-dimensional bulk, the brane geometry is trivial, as are the corresponding energies. The Casimir effect may then be the only mechanism available to stabilize the brane’s location in this case.

In summary, the gradients of the total energy result in a net *force*, which can stabilize the location of a brane. In this work, we generalize the results of [17], confining our attention to a codimension-1 brane wrapped around either the 2-dimensional hyperbolic horn or the Euclidean cone, but extending our analysis to additionally include the Neumann boundary condition, as well as analogous calculations in $D = 2 + 1$ (i.e without the Minkowski dimensions). On both geometries (in $D = 5 + 1$) we suppose that all Standard Model fields are confined to a codimension-1 brane as pictured in Figure 2 or 7, but that they are free to propagate in the compact (i.e. “universal” [18]) dimension. This is possible if the “circumference” of the brane is small enough so that the first excited “Kaluza Klein” mode has not yet been made accessible by experiment.

We have calculated the total energy of these systems as the sum of tension and elastic energies (i.e. those local to the brane and associated with its geometry) as well as the (global) vacuum energy from a bulk scalar field, ϕ , that satisfies a boundary condition on the brane. We also parametrize the vacuum energy of Standard Model fields confined on the brane. For each geometry, we first consider total space-time dimension $D = 2 + 1$ then consider the addition of three Minkowski dimensions in $D = 5 + 1$. While the 2+1 D cases are interesting for academic reasons, they also illuminate how the different contributions

to the brane potential scale differently with the number of spatial dimensions as well as provide examples of the how the explicit poles of the vacuum energy depend significantly on the even/oddness of D .

In section II we analyze the hyperbolic horn, considering both dimensionalities and boundary conditions. There we discover, in both dimensionalities, that a competition between tension and bulk Casimir energies can result in a stable brane position, however only for the Dirichlet case. In Section III we perform the analogous calculations for the cone. A stable minimum is possible for all boundary conditions in $D = 2 + 1$ and can result from the competition between the tension and elastic energies (i.e. purely from geometric effects), but is also ensured by the Casimir energy from the scalar. In $D = 5 + 1$ a global minimum occurs for the Dirichlet case while only a local minimum is possible for Neumann. In Section IV we conclude with a summary of results and discussion.

II. HYPERBOLIC HORN

A. Preliminaries

1. The Model, Energy Contributions, and Bulk ϕ Solutions

Here we will consider a general spacetime dimension $D = m + 2 + 1$, where m indicates the number of Minkowski spatial dimensions. That is, the the full spacetime manifold is $\mathcal{M}^{m+1} \times \mathcal{H}^2/\Gamma$. The line element can be written in coordinates such that

$$ds^2 = \eta_{\mu\nu}^{(m+1)} dx^\mu dx^\nu + e^{-2z/z_*} z_*^2 d\theta^2 + dz^2,$$

where we identify $(\theta) \leftrightarrow (\theta + 2\pi)$, and we have chosen our coordinates such that the horn circumference at $z = 0$ is $2\pi z_*$. Furthermore, from here on we shall work in units where the intrinsic length scale of the horn, $z_* \equiv 1$. The model is illustrated in Figure 2, suppressing any Minkowski spatial dimensions, where the codimension-1 brane wraps around the compact direction and resides at coordinate z_b . In $D = 5 + 1$ ($m = 3$) we assume the Standard Model fields to be confined to the brane, free to propagate in the compact direction. We will now enumerate different contributions to the brane's effective potential on the horn.

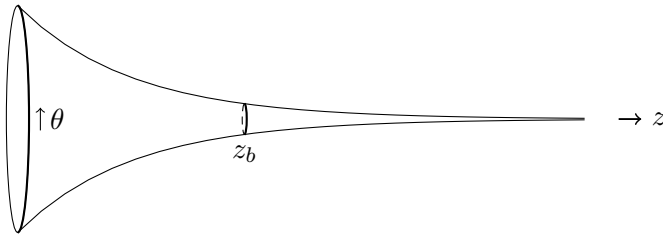


FIG. 2: A partial embedding diagram of the horn. The codimension-1 brane is pictured with coordinate z_b . The manifold is infinite in extent in the $\pm z$ directions.

Energy Contributions

There will be a contribution from a non-zero brane tension, σ , that provides an energy

$$E_{\text{ten}} = \int d^{1+m}x \sqrt{|\gamma|} \sigma = 2\pi e^{-z_b} V_M \sigma, \quad (1)$$

where $\gamma_{\mu\nu}$ is the induced spatial metric on the brane, and the volume of the regulated Minkowski spatial slice is denoted by V_M . There will also be an “elastic” energy contribution due to the extrinsic curvature of the brane, K_{ab} (see Appendix E 2 a). We write this as an expansion in scalars built from K_{ab} , namely

$$E_{\text{curv}} = \int d^{1+m}x \sqrt{|\gamma|} (h_1 K^2 + h_2 K_{ab} K_{ab} + \dots) = 2\pi e^{-z_b} V_M (h_1 + h_2 + \dots) \quad (2)$$

where the h_i are parameters describing the energy cost for deforming the brane within the manifold, and \dots represents other possible scalars^[3] that are higher order in K_{ab} . Note that the effect of σ and the h_i are completely indistinguishable, at least as far as the total energy of the system is concerned. Without loss of generality, then, we shall set $h_i = 0$ and encode all geometric effects in σ . It is already clear that these effects behave monotonically with z_b , and are thus insufficient to stabilize the brane by themselves, but as we will see, the Casimir energies from the brane or bulk can provide a complementary opposing force.

[3] In principle we should also include possible coupling between the extrinsic- and Riemann curvature tensors, however in this geometry those terms appear with the same z_b -dependence, thus at this level they are indistinguishable from the terms with only extrinsic curvature.

The Casimir (or vacuum) energy in the bulk scalar ϕ on a constant- t hypersurface is

$$E_0 = \int \sqrt{-g} d\Sigma \langle 0 | T_{00}^{(\phi)} | 0 \rangle \quad (3)$$

from which one obtains the canonical result $E_0 = \frac{1}{2} \sum_{\mathbf{i}} \omega_{\mathbf{i}}$, where \mathbf{i} is a general mode index. It is well known that this sum is infinite; to extract the physically relevant energy we employ the zeta-function regularization technique (see e.g. [19]) and write

$$E_0(s) = \frac{\mu^{2s}}{2} \sum_{\mathbf{i}} \omega_{\mathbf{i}}^{1-2s} \quad (4)$$

where μ is a renormalization scale. The generalized sum is finite for large enough s , which is analytically continued to zero. In some systems the terms in the energy that determine the Casimir *force* remain finite even in the limit $s \rightarrow 0$, while in others they diverge and must be dealt with explicitly; in either case it is ultimately the renormalization of geometric parameters in the full theory (including gravity) that remedies the situation.

In the $D = 5 + 1$ model there will also be a vacuum energy associated with the Standard Model fields living on the brane, sensitive to the size of the brane in the compact dimension. Though we will not calculate this effect explicitly, by dimensional considerations we expect its associated 4D energy density to scale approximately inversely proportional to the fourth power of this length scale, namely

$$\rho_{0,SM} \simeq \frac{\kappa_{SM}}{(2\pi e^{-z_b})^4} \quad (5)$$

where κ_{SM} is a dimensionless coefficient (recall that we are working in units where $z_* \equiv 1$).

Bulk ϕ Solutions

The action for a real massless scalar field in D space-time dimensions is

$$S_\phi = \frac{1}{2} \int d^D x \sqrt{-g} \nabla_\mu \phi \nabla^\mu \phi \quad (6)$$

whose variation with respect to ϕ yields the Klein-Gordon equation on this space-time,

$$\square \phi = (-\partial_t^2 + \nabla^2) \phi = 0 \quad (7)$$

where

$$\nabla^2 = \nabla_{\mathbf{x}}^2 + e^{2z} \frac{\partial^2}{\partial \theta^2} + \frac{\partial^2}{\partial z^2} - \frac{\partial}{\partial z} \quad (8)$$

and $\nabla_{\mathbf{x}}^2$ is the Minkowski-space Laplacian. The positive frequency modes, $u_{\mathbf{i}}$, are

$$u_{\mathbf{i}} = A_{\mathbf{i}} e^{-i(\omega t - \mathbf{p} \cdot \mathbf{x} - n\theta)} Z_{n,k}(z), \quad (9)$$

where $n \in \mathbb{Z}$ and $A_{\mathbf{i}}$ is a normalization constant. $Z_{n,k}$ satisfies

$$Z_{n,k}''(z) - Z_{n,k}'(z) + (\omega^2 - p^2 - n^2 e^{2z}) Z_{n,k}(z) = 0, \quad (10)$$

where $p = |\mathbf{p}|$ is the momentum in the Minkowski directions. We find that the boundary conditions and normalizability imply a real $k > 0$, defined by the dispersion relation

$$\omega = \sqrt{p^2 + k^2 + \frac{1}{4}} \quad (11)$$

To make the problem more tractable, we regulate the infinite spatial volume of the horn by truncating the space at $z = z_L$, where $z_L < z_b$, and impose there a Dirichlet boundary condition on the field^[4]. At the appropriate place in the calculation we take the limit $z_L \rightarrow -\infty$ to recover the full horn spacetime. For the $n \neq 0$ modes we find (see Appendix A 1)

$$Z_{n \neq 0, k} = \begin{cases} e^{z/2} [I_{-ik}(|n|e^{z_L}) I_{ik}(|n|e^z) - I_{ik}(|n|e^{z_L}) I_{-ik}(|n|e^z)] & \text{when } z_L \leq z \leq z_b, \\ e^{z/2} K_{ik}(|n|e^z) & \text{when } z_b \leq z. \end{cases} \quad (12)$$

The $n = 0$ modes do not contribute to the Casimir force, as we show explicitly in Appendix B 3; however this can be understood from the following argument. From (10) we see that these solutions behave as $e^{z/2} \sin k(z - z_{L,R})$, and the energy density *per unit* z in these modes is proportional to $\sqrt{|g|} Z_{0,k}^2 = \sin^2 k(z - z_{L,R})$, where z_L and z_R are simply there to temporarily regulate the size of the space in the z -direction. This is the same form as the energy density of scalar modes in a 1-dimensional box; as the box size goes to infinity we know there is no Casimir force due to translation invariance. Thus the $n = 0$ modes on the horn do not contribute to the Casimir force, essentially, because they don't "feel" that translation invariance of the manifold is broken.

[4] This makes the modes discrete and normalizable. The choice of Dirichlet boundary condition is arbitrary and should have no bearing on the end result.

For all n , the spectrum of k are determined by the boundary conditions at z_b :

$$0 = \begin{cases} Z_{n,k}(z_b) & \text{(Dirichlet),} \\ \text{or} \\ Z'_{n,k}(z_b) & \text{(Neumann).} \end{cases} \quad (13)$$

Finally, the field ϕ may be expanded in terms of the solutions as

$$\phi = \sum_{\mathbf{i}} a_{\mathbf{i}} u_{\mathbf{i}} + a_{\mathbf{i}}^{\dagger} u_{\mathbf{i}}^*, \quad (14)$$

where $a_{\mathbf{i}}^{\dagger}$ and $a_{\mathbf{i}}$ are the creation and annihilation operators of modes labeled by the set of quantum numbers, \mathbf{i} . As usual, the vacuum state is defined as $a_{\mathbf{i}} |0\rangle = 0$ and the operators satisfy the commutation relations, $[a_{\mathbf{i}}, a_{\mathbf{j}}] = 0 = [a_{\mathbf{i}}^{\dagger}, a_{\mathbf{j}}^{\dagger}]$, and $[a_{\mathbf{i}}, a_{\mathbf{j}}^{\dagger}] = \delta_{\mathbf{ij}}$. The positive-energy eigenfunctions are normalized using the Klein-Gordon norm (assuming a discrete spectrum):

$$(u_{\mathbf{i}}, u_{\mathbf{j}}) \equiv i \int \sqrt{-g} d\Sigma n^{\mu} (u_{\mathbf{i}}^* \nabla_{\mu} u_{\mathbf{j}} - u_{\mathbf{j}} \nabla_{\mu} u_{\mathbf{i}}^*) \equiv \delta_{\mathbf{ij}} \quad (15)$$

where Σ is a spacelike hypersurface, and n^{μ} is a unit timelike vector normal to it.

2. Procedure for Calculation of Casimir Energy on the Horn

Contour Integral Representation of Sum

As we generally have no explicit expression for the $\{k\}$, we will calculate (4) in part using a contour integral representation, as elucidated in [19]. To this end, the following will be of use for both the $D = 2+1$ and $5+1$ models (i.e. $m = 0$ and $m = 3$):

$$\sum_{\{k\}} \left(k^2 + \frac{1}{4}\right)^{\frac{(m+1)}{2}-s} = \frac{1}{2\pi i} \oint_{\gamma} dk \left(k^2 + \frac{1}{4}\right)^{\frac{(m+1)}{2}-s} \frac{\partial}{\partial k} \ln \Delta_n(k) \quad (16)$$

where γ is a counter-clockwise contour that encloses the entire spectrum (the positive real axis) and $\Delta_n(k)$ are appropriate mode-generating functions whose roots correspond to our spectrum of k (for details see Appendix B, or e.g. references [19] or [20]). With properly

chosen generating functions, one can show that the contour may be deformed to give

$$\sum_{\{k\}} \left(k^2 + \frac{1}{4}\right)^{\frac{(m+1)}{2}-s} = -\frac{\cos \pi \left(\frac{m}{2} - s\right)}{\pi} \int_{1/2}^{\infty} dk \left(k^2 - \frac{1}{4}\right)^{\frac{(m+1)}{2}-s} \frac{\partial}{\partial k} \ln \Delta_n(ik) \quad (17)$$

We have derived a set of mode generating functions for $n \neq 0$ and $n = 0$ separately (Appendix B), and have shown that the $n = 0$ modes are independent of z_b , and so *we omit $n = 0$ from any sums we encounter*. We find the mode generating functions for both sides of z_b to effectively combine to give the log of the total generating functions

$$\ln \Delta_n(ik) = \begin{cases} \ln [IK] & \text{(Dirichlet),} \\ \ln \left[\frac{1}{4}IK + \frac{1}{2}x_b(I'K + IK') + x_b^2 I'K'\right] & \text{(Neumann),} \end{cases} \quad (18)$$

where, for brevity, we denote $I_k(|n|e^{z_b})$ by I and $K_k(|n|e^{z_b})$ by K , and $'$ denotes a derivative with respect to the argument of the Bessel function. Any z_b -independent terms have been omitted as they do not contribute to the Casimir force.

General Analysis of $E_0(s)$

The divergent piece from $E_0(s)$ needs to be separated out so that its physically relevant part may be revealed through an analytic continuation in s , else the divergent quantities need to be explicitly absorbed through some renormalization of parameters in the full theory. Because the summand is even in n and $n = 0$ isn't counted, we may take

$$\sum_n \rightarrow 2 \sum_{n=1}^{\infty} \quad (19)$$

so that in general we have

$$E_0(s) \propto \sum_{n=1}^{\infty} \int_{1/2}^{\infty} dk \left(k^2 - \frac{1}{4}\right)^{\frac{(m+1)}{2}-s} \frac{\partial}{\partial k} \ln \Delta_n(ik) \quad (20)$$

Given (18), an analytic continuation of (20) in s is impossible in its current form, so we approach it using a uniform asymptotic expansion, closely following the procedure in [19]. We know the divergences occur at large k and n , but the idea is to isolate their asymptotic behavior, taking them to infinity simultaneously while keeping their ratio fixed. If this asymptotic behavior can be understood analytically, it is then straightforward to handle the

divergent contributions so that the remaining finite part may be calculated numerically. To this end, we decompose $E_0(s)$ into a sum of its asymptotic and finite part:

$$E_0(s) \equiv E_0^{\text{as}}(s) + E_0^{\text{fin}} \quad (21)$$

We change variables, defining

$$x_b \equiv |n|e^{z_b} \quad (22)$$

and

$$y \equiv \frac{k}{x_b}. \quad (23)$$

Our sum/integral therefore becomes

$$E_0(s) \propto \sum_{n=1}^{\infty} x_b^{m+1-2s} \int_{(2x_b)^{-1}}^{\infty} dy \left(y^2 - \frac{1}{4x_b^2} \right)^{\frac{(m+1)}{2}-s} \frac{\partial}{\partial y} \ln \Delta_n(iyx_b). \quad (24)$$

From the uniform asymptotic behavior of the two modified Bessel functions (see e.g. [21]), we define the asymptotic part of the log of the generating function as

$$\tilde{\ln}[\Delta_n(iyx_b)] \equiv \ln \left[\frac{1}{2x_b \sqrt{y^2 + 1}} \right] + \sum_{j=1}^{m+2} \frac{f_j(y^{-1})}{(yx_b)^j} \quad (\text{Dirichlet}) \quad (25)$$

$$\equiv \ln \left[-\frac{x_b}{2} \sqrt{y^2 + 1} \right] + \sum_{j=1}^{m+2} \frac{g_j(y^{-1})}{(yx_b)^j} \quad (\text{Neumann}), \quad (26)$$

where the $f_j(z)$ and $g_j(z)$ are rational functions of z , given in Appendix C. We find it most convenient to capture the divergences of (24) by defining^[5]

$$E_0^{\text{as}}(s) \propto \sum_{n=1}^{\infty} x_b^{m+1-2s} \int_{(2x_b)^{-1}}^{\infty} dy \left(y^2 - \frac{1}{4x_b^2} \right)^{\frac{(m+1)}{2}-s} \frac{\partial}{\partial y} \tilde{\ln}[I_{yx_b}(x_b) K_{yx_b}(x_b)]. \quad (27)$$

for the Dirichlet case, and similarly for Neumann. We will see that the integral may be performed analytically, however the sum must be done numerically and so an analytic continuation again becomes challenging. We will then find it convenient to further decompose $E_0^{\text{as}}(s)$ into divergent and ‘‘remainder’’ parts, $E_0^{\text{div}}(s)$ and E_0^{rem} . In summary, the total energy (or energy density) of the system will be given by

$$E = E_{\text{ten}} + E_0^{\text{div}}(s) + E_0^{\text{rem}} + E_0^{\text{fin}} \quad (D = 2 + 1) \quad (28)$$

$$\rho = \rho_{\text{ten}} + \rho_0^{\text{div}}(s) + \rho_0^{\text{rem}} + \rho_0^{\text{fin}} + \rho_{0, \text{SM}} \quad (D = 5 + 1) \quad (29)$$

[5] This turns out to be easier than doing an expansion in inverse powers of x_b of the entire integrand.

B. $D = 2 + 1$

Here there are no Minkowski dimensions, so $\mathbf{p} = 0$. From (4) and (17) we have

$$E_0(s) = -\frac{\mu^{2s}}{\pi} \cos \pi s \sum_{n=1}^{\infty} \int_{1/2}^{\infty} dk \left(k^2 - \frac{1}{4}\right)^{1/2-s} \frac{\partial}{\partial k} \ln \Delta_k(ik) \quad (30)$$

where $\ln \Delta_n(ik)$ is defined by (18) in both the Dirichlet and Neumann cases.

1. *Dirichlet Condition*

Many of the details of this section are included in Appendix D and maybe be easily generalized to the other cases. Considering (25) and (27), we define the asymptotic part of the energy as

$$E_0^{\text{as}}(s) = -\frac{\mu^{2s}}{\pi} \cos \pi s \sum_{n=1}^{\infty} x_b^{1-2s} \int_{(2x_b)^{-1}}^{\infty} dy \left(y^2 - \frac{1}{4x_b^2}\right)^{1/2-s} \frac{\partial}{\partial y} \tilde{\ln}[I_{yx_b}(x_b) K_{yx_b}(x_b)] \quad (31)$$

After analytically continuing towards $s = 0$ we find

$$E_0^{\text{as}}(s) = -\frac{(2\mu)^{2s}}{4} \cos \pi s \sum_{n=1}^{\infty} \frac{1 + 16x_b^2 + (49 - 10s)x_b^4 + 64x_b^6}{(1 + 4x_b^2)^{5/2+s}} \quad (32)$$

As $x_b \propto n$, the divergences here will come from the terms in the summand that go asymptotically as x_b or x_b^{-1} ; we extract these by defining

$$E_0^{\text{as}}(s) \equiv E_0^{\text{div}}(s) + E_0^{\text{rem}} \quad (33)$$

where we have expanded in inverse powers of x_b to obtain

$$\begin{aligned} E_0^{\text{div}}(s) &= -\mu^{2s} \cos \pi s \sum_{n=1}^{\infty} \left(\frac{1}{2} x_b^{1-2s} + \frac{9-26s}{128} x_b^{-1-2s} \right) \\ &= \frac{e^{z_b}}{24} + \frac{9}{128} e^{-z_b} \left(\frac{13}{9} - \gamma - \frac{1}{2s} - \ln[\mu e^{-z_b}] \right) \end{aligned} \quad (34)$$

and (evaluated with $s = 0$)

$$E_0^{\text{rem}} = \sum_{n=1}^{\infty} \left[-\frac{1 + 16x_b^2 + 49x_b^4 + 64x_b^6}{4(1 + 4x_b^2)^{5/2}} + \left(\frac{1}{2} x_b + \frac{9}{128} x_b^{-1} \right) \right] \quad (35)$$

Asymptotically, we find

$$E_0^{\text{rem}} \sim \begin{cases} -\frac{7+36 \ln 2}{256} \times e^{-z_b} & \text{as } z_b \rightarrow -\infty, \\ -\frac{23}{1024} \zeta(3) \times e^{-3z_b} & \text{as } z_b \rightarrow +\infty. \end{cases} \quad (36)$$

where we have used a lowest order Euler-Maclauren expansion in the first line, and a Taylor expansion in x_b^{-1} in the second. After setting $s = 0$, integrating by parts^[6], and returning to the variables k and x_b one arrives at

$$E_0^{\text{fin}} = \frac{1}{\pi} \sum_{n=1}^{\infty} \int_{1/2}^{\infty} dk \frac{k}{(k^2 - \frac{1}{4})^{1/2}} \left(\ln [I_k(x_b) K_k(x_b)] - \tilde{\ln}[I_k(x_b) K_k(x_b)] \right) \quad (37)$$

Asymptotically, we find

$$E_0^{\text{fin}} \sim \begin{cases} 2.4 \times 10^{-3} \times e^{-z_b} & \text{as } z_b \rightarrow -\infty, \\ -1.4 \times 10^{-3} \times e^{-3z_b} & \text{as } z_b \rightarrow +\infty. \end{cases} \quad (38)$$

We have learned that E_0^{div} contains an explicit $1/s$ pole which is proportional to e^{-z_b} ; we have also verified this using a complementary heat kernel analysis (see Appendix E). The presence of the pole and the arbitrary scale μ is indicative of the fact that the Casimir energy cannot be measured in isolation; it is only a contribution to a total energy that is itself finite [22]. One must identify a parameter that is to be renormalized – since this offending term is proportional to the brane length, a renormalization of the brane tension will suffice, with μ setting the renormalization scale. In so doing, we choose to go beyond minimal subtraction and absorb finite corrections into the tension as well, hence we find the asymptotic behaviors (see Appendix D)

$$E(z_b) \sim \begin{cases} 2\pi z_* e^{-z_b/z_*} \times \sigma_{\text{ren}} & \text{as } z_b \rightarrow -\infty, \\ \frac{1}{24} \frac{e^{z_b/z_*}}{z_*} & \text{as } z_b \rightarrow +\infty. \end{cases} \quad (39)$$

where we have restored the horn length scale, z_* . We find that the total energy is unbounded from above as $z_b \rightarrow +\infty$ and likewise for $z_b \rightarrow -\infty$ as long as $\sigma_{\text{ren}} > 0$, and therefore a global minimum exists. $E(z_b)$ is plotted in Figure 3.

[6] This is advisable for numerical purposes.

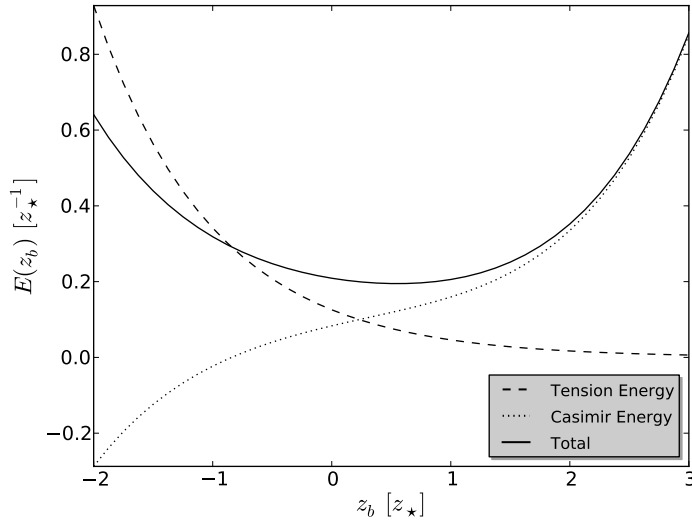


FIG. 3: In $D = 2 + 1$ with a Dirichlet boundary condition on ϕ , various potential contributions as a function of z_b . For illustration we have chosen $\sigma_{\text{ren}} = 0.02 [z_*^{-2}]$.

2. Neumann Condition

Here we repeat the analysis of the previous section, only now using the Neumann specification in (18). Altogether, we find the asymptotic behaviors

$$E(z_b) \sim \begin{cases} 2\pi z_* e^{-z_b/z_*} \times \sigma_{\text{ren}} & \text{as } z_b \rightarrow -\infty, \\ -\frac{1}{24} \frac{e^{z_b/z_*}}{z_*} & \text{as } z_b \rightarrow +\infty. \end{cases} \quad (40)$$

We find that the Casimir energy is unbounded from below for $z_b \rightarrow +\infty$ (the sign of the energy is flipped with respect to the Dirichlet case, in this limit), and brane tension cannot compensate for this, therefore no stabilizing mechanism exists in this case. $E(z_b)$ is plotted in Figure 4 without brane tension.

C. $D = 5 + 1$

Here the previous analysis is repeated, adding three Minkowski spatial dimensions, i.e. $m = 3$. For ease of normalization we compactify these dimensions using a torus of fundamental side length, $V_M^{1/3}$, which is taken to infinity to recover a true global Minkowski

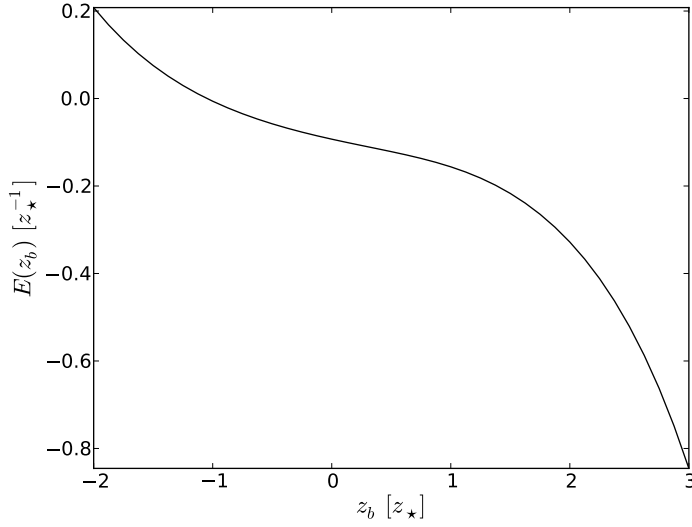


FIG. 4: In $D = 2 + 1$ with a Neumann boundary condition, the total energy as function of z_b . Here we have chosen $\sigma_{\text{ren}} = 0$.

space. In this limit, the Minkowski momentum, \mathbf{p} , becomes continuous. The sum over the components of \mathbf{p} turns into an integral as

$$\sum_{\mathbf{p}} = \sum_{\mathbf{p}} \frac{\Delta p_x}{2\pi/V_M^{1/3}} \frac{\Delta p_y}{2\pi/V_M^{1/3}} \frac{\Delta p_z}{2\pi/V_M^{1/3}} \rightarrow \frac{V_M}{(2\pi)^3} \int dp_x dp_y dp_z = \frac{V_M}{2\pi^2} \int dp p^2 \quad (41)$$

From (4) we now have the effective 4D vacuum energy

$$\rho_0(s) = \frac{\mu^{2s}}{2\pi^2} \sum_{n=1}^{\infty} \sum_{\{k\}} \int dp p^2 \left(p^2 + k^2 + \frac{1}{4} \right)^{1/2-s} \quad (42)$$

We compute the p -integral by first performing a Mellin transform,

$$\left(p^2 + k^2 + \frac{1}{4} \right)^{1/2-s} = \int_0^{\infty} dt \frac{t^{s-3/2}}{\Gamma(s-1/2)} e^{-t(p^2+k^2+\frac{1}{4})} \quad (43)$$

which allows us to directly integrate over p , yielding

$$\rho_0(s) = \frac{\mu^{2s}}{8\pi^{3/2}} \frac{\Gamma(s-2)}{\Gamma(s-1/2)} \sum_{n=1}^{\infty} \sum_{\{k\}} \left(k^2 + \frac{1}{4} \right)^{2-s} \quad (44)$$

We now represent the sum over $\{k\}$ as a contour integral using (17), giving

$$\begin{aligned}\rho_0(s) &= \frac{\mu^{2s}}{8\pi^{5/2}} \frac{\Gamma(s-2) \sin \pi s}{\Gamma(s-1/2)} \sum_{n=1}^{\infty} \int_{1/2}^{\infty} dk \left(k^2 - \frac{1}{4}\right)^{2-s} \frac{\partial}{\partial k} \ln \Delta_n(ik) \\ &= -\frac{\mu^{2s}}{32\pi^2} \left(1 + s \left(\frac{3}{2} - \gamma - \psi(-1/2)\right)\right) \sum_{n=1}^{\infty} \int_{1/2}^{\infty} dk \left(k^2 - \frac{1}{4}\right)^{2-s} \frac{\partial}{\partial k} \ln \Delta_n(ik)\end{aligned}\quad (45)$$

where ψ is the Digamma function, and we have omitted terms higher order in s as they vanish in the $s \rightarrow 0$ limit.

1. Dirichlet Condition

Considering (25) and (27) we define

$$\begin{aligned}\rho_0^{\text{as}}(s) &= -\frac{\mu^{2s}}{32\pi^2} \left(1 + s \left(\frac{3}{2} - \gamma - \psi(-1/2)\right)\right) \sum_{n=1}^{\infty} x_b^{4-2s} \int_{(2x_b)^{-1}}^{\infty} dy \left(y^2 - \frac{1}{4x_b^2}\right)^{2-s} \\ &\quad \times \frac{\partial}{\partial y} \tilde{\ln}[I_{yx_b}(x_b) K_{yx_b}(x_b)]\end{aligned}\quad (46)$$

The integral may be performed analytically, yielding a cumbersome expression which we omit for brevity. Here the divergences come from terms in the summand that behave asymptotically as x_b^4, x_b^2 or x_b^0 . We isolate those terms in (having already performed the sum on n)

$$\rho_0^{\text{div}}(s) = \frac{1}{2048\pi^2} \left(-\frac{47}{12} + \gamma - \frac{1}{s} - 2 \ln \pi \mu e^{-z_b} + \psi(-1/2)\right) - \frac{3}{64\pi^2} \zeta'(-2) e^{2z_b} + \frac{1}{32\pi^2} \zeta'(-4) e^{4z_b}\quad (47)$$

From this we numerically obtain

$$\rho_0^{\text{rem}} = \lim_{s \rightarrow 0} (\rho_0^{\text{as}}(s) - \rho_0^{\text{div}}(s))\quad (48)$$

which asymptotically behaves as

$$\rho_0^{\text{rem}} \sim \begin{cases} -1.5 \times 10^{-4} \times e^{-z_b} & \text{as } z_b \rightarrow -\infty, \\ 6.8 \times 10^{-5} \times e^{-2z_b} & \text{as } z_b \rightarrow +\infty. \end{cases}\quad (49)$$

Lastly, we return to the variables k, x_b and integrate by parts to give

$$\rho_0^{\text{fin}} = \frac{1}{8\pi^2} \sum_{n=1}^{\infty} \int_{1/2}^{\infty} dk k \left(k^2 - \frac{1}{4}\right) \left(\ln [I_k(x_b) K_k(x_b)] - \tilde{\ln}[I_k(x_b) K_k(x_b)]\right),\quad (50)$$

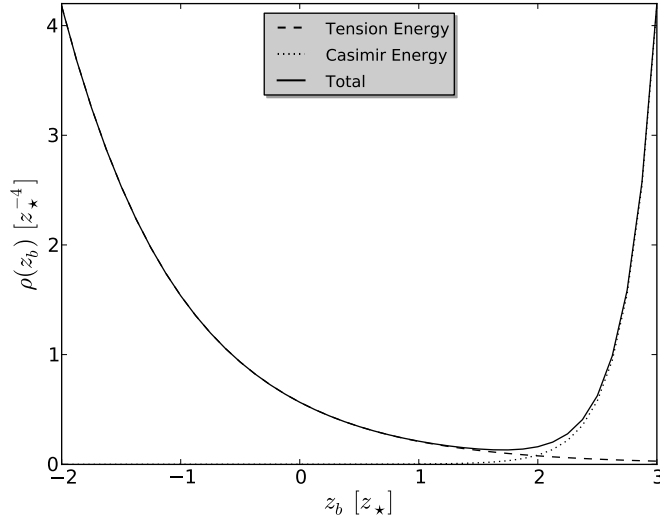


FIG. 5: For $D = 5 + 1$ with the Dirichlet condition on ϕ , the total 4D energy density in units of the horn curvature scale (z_*), as a function of the brane position, z_b . For illustration, we have taken the brane tension, $\sigma_{\text{ren}} = 0.09 [z_*^{-5}]$, and $\kappa_{SM} = 0$.

Asymptotically, one may show

$$\rho_0^{\text{fin}} \sim \begin{cases} -2.0 \times 10^{-5} \times e^{-z_b} & \text{as } z_b \rightarrow -\infty, \\ 4.4 \times 10^{-5} \times e^{-2z_b} & \text{as } z_b \rightarrow +\infty. \end{cases} \quad (51)$$

In contrast to the 2+1 case, the pole in $E_0^{\text{div}}(s)$ is a constant and is simply discarded. Altogether we have the asymptotic behaviors

$$\rho(z_b) \sim \begin{cases} 2\pi z_* e^{-z_b/z_*} \times \sigma_{\text{ren}} & \text{as } z_b \rightarrow -\infty, \\ \frac{1}{16\pi^4 z_*^4} \left(\frac{1}{2}\pi^2 \zeta'(-4) + \kappa_{SM} \right) \times e^{4z_b/z_*} & \text{as } z_b \rightarrow +\infty. \end{cases} \quad (52)$$

where finite quantum corrections have been absorbed by σ_{ren} , and $1/2\pi^2\zeta'(-4) \approx 0.04$. As in the $D = 2 + 1$ case, here there is a global minimum, assuming $\sigma_{\text{ren}} > 0$ and assuming the value of κ_{SM} doesn't alter these results (see Figure 5). For $\sigma = \mathcal{O}(1) [z_*^{-5}]$, the effective mass for the brane's position modulus is $\mathcal{O}(z_*^{-1})$.

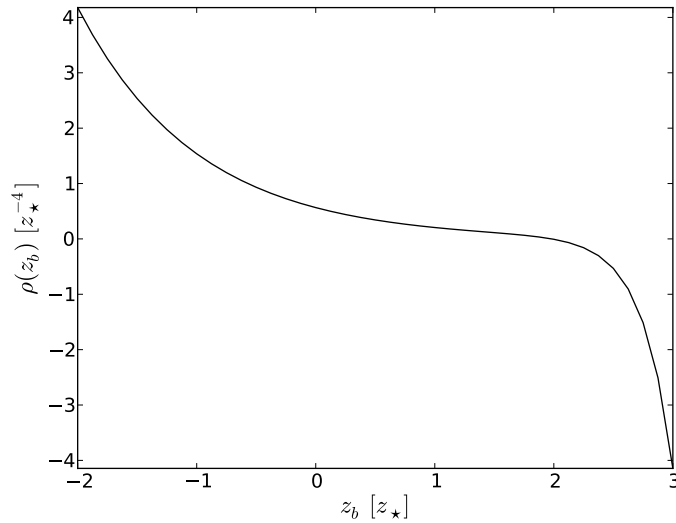


FIG. 6: For $D = 5 + 1$ with the Neumann condition on ϕ , the total 4D energy density in units of the horn curvature scale (z_*), as a function of the brane position, z_b . Here we have chosen $\sigma_{\text{ren}} = 0$, and $\kappa_{SM} = 0$.

2. Neumann Condition

Here we proceed as in the previous section, only using (26). Altogether we find the asymptotic behaviors

$$\rho(z_b) \sim \begin{cases} 2\pi z_* e^{-z_b/z_*} \times \sigma_{\text{ren}} & \text{as } z_b \rightarrow -\infty, \\ \frac{1}{16\pi^4 z_*^4} \left(-\frac{1}{2}\pi^2 \zeta'(-4) + \kappa_{SM} \right) \times e^{4z_b/z_*} & \text{as } z_b \rightarrow +\infty. \end{cases} \quad (53)$$

Once again, the sign of the vacuum energy in ϕ is flipped with respect to the Dirichlet case in the $z_b \rightarrow \infty$ limit. It is thus unbounded from below, and no value of brane tension can create a stable minimum, however a sufficiently large and positive κ_{SM} would accomplish this (see Figure 6).

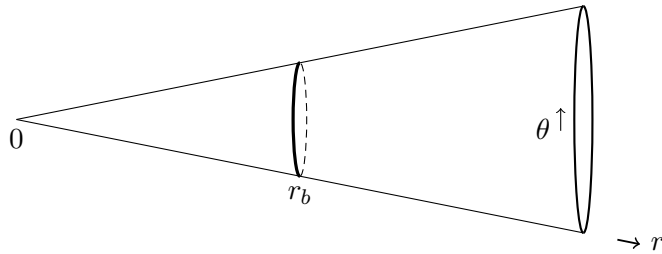


FIG. 7: A partial embedding diagram of the cone. The brane is pictured at coordinate r_b . As opposed to the horn, this manifold is geometrically flat and is infinite in extent only in one direction.

III. EUCLIDEAN CONE

A. Preliminaries

1. The Model, Energy Contributions, and Bulk ϕ Solutions

Once more we work in general spacetime dimension $D = m + 2 + 1$, where m indicates the number of Minkowski spatial dimensions. That is, the topology of the full spacetime manifold is $\mathcal{M}^{m+1} \times (\mathbb{R}^2 - \{0\})$. The line element can be written in coordinates such that

$$ds^2 = \eta_{\mu\nu}^{(m+1)} dx^\mu dx^\nu + dr^2 + r^2 d\theta^2$$

where we identify $\theta \leftrightarrow \theta + 2\pi(1 - \delta)$, i.e. the conical space is defined by the deficit angle $2\pi\delta$. Again, a 1-brane (4-brane) is wrapped around this space in $D = 2 + 1$ ($D = 5 + 1$) and resides at coordinate distance r_b away from the cone tip, as illustrated in Figure 7. As opposed to the horn, the cone is flat, having no intrinsic length scale associated with it.

Energy Contributions

Here, a non-zero brane tension (σ) contributes an energy given by

$$E_{\text{ten}} = \int d^{1+m}x \sqrt{|\gamma|} \sigma = 2\pi(1 - \delta) r_b V_M \sigma \quad (54)$$

where $\gamma_{\mu\nu}$ is the induced spatial metric on the brane, while the elastic energy characterized

by the extrinsic curvature of the brane, K_{ab} (see Appendix E 2 b) is

$$E_{\text{curv}} = \int d^{1+m}x \sqrt{|\gamma|} (h_1 K^2 + h_2 K_{ab} K_{ab} + \dots) = \frac{2\pi(1-\delta)}{r_b} V_M (h_1 + h_2 + \dots) \quad (55)$$

where the h_i are parameters describing the energy cost for deforming the brane within the manifold, and \dots represents other possible scalars^[7] that are built from terms higher order in K_{ab} . Note that the effect of each of these terms is completely indistinguishable from one another, at least as far as the total energy of the system is concerned. Without loss of generality, then, we shall define $h_1 + h_2 + \dots \equiv h$. As opposed to the horn, the tension and elastic energies appear with markedly different dependences on the brane location. Interestingly, it is already apparent that these two energies are sufficient to stabilize the brane under the physically reasonable assumption that $\sigma, h > 0$.

The zero-point energy in the bulk ϕ is again zeta-function regularized and is given by (4). As we will see below, a check on our results is available in $D = 2 + 1$ when $\delta = 0$ as this is simply the Casimir effect of the 1-sphere. In $D = 5 + 1$ we parametrize the vacuum energy of brane-dwelling Standard Model fields, from dimensional considerations, by

$$\rho_{0, \text{SM}} \simeq \frac{\kappa_{SM}}{(2\pi(1-\delta)r_b)^4} \quad (56)$$

where κ_{SM} is a dimensionless coefficient.

Bulk ϕ Solutions

Again, the massless bulk scalar field obeys the Klein-Gordon equation,

$$\square\phi = (-\partial_t^2 + \nabla^2)\phi = 0 \quad (57)$$

where

$$\nabla^2 = \nabla_{\mathbf{x}}^2 + \frac{\partial^2}{\partial r^2} + \frac{1}{r} \frac{\partial}{\partial r} + \frac{1}{r^2} \frac{\partial^2}{\partial \theta^2} \quad (58)$$

and $\nabla_{\mathbf{x}}^2$ is the Minkowski-space Laplacian. The positive frequency modes, $u_{\mathbf{i}}$, are found to be

$$u_{\mathbf{i}} = A_{\mathbf{i}} e^{-i(\omega t - \mathbf{p} \cdot \mathbf{x} - \nu \theta)} R_{n,k}(r) \quad (59)$$

[7] Coupling to the Riemann curvature tensor is trivial as it is zero for this geometry.

where $\nu \equiv n/(1 - \delta)$, $n \in \mathbb{Z}$, A_i is a normalization constant, and $R_{n,k}$ satisfies Bessel's equation

$$R''_{n,k}(r) + \frac{1}{r}R'_{n,k}(r) + \left(k^2 - \frac{\nu^2}{r^2}\right)R_{n,k}(r) = 0 \quad (60)$$

whose solutions may be written as a linear combination of the Bessel functions of the first and second kind, $J_\nu(kr)$ and $N_\nu(kr)$, or the Hankel functions $H_\nu^{(1)}(kr)$ and $H_\nu^{(2)}(kr)$. The positive frequency dispersion relation is

$$\omega = \sqrt{p^2 + k^2} \quad (61)$$

where $p = |\mathbf{p}|$ is the momentum in the Minkowski directions. Note that while ω doesn't have an explicit n -dependence, the quantized k 's do depend on n non-trivially.

To make the problem more tractable, we regulate the infinite spatial volume of the cone by truncating the space at an outer coordinate $r_{\text{out}} \gg r_b$, and impose there a Dirichlet boundary condition on the field. At the appropriate place in the calculation we take the limit $r_{\text{out}} \rightarrow +\infty$ to recover the full spacetime.

For the interior solutions we use Bessel functions and find that for $n \neq 0$ the only ones that are normalizable are

$$R_{n \neq 0, k}(r) = J_\nu(kr) \quad (0 \leq r \leq r_b) \quad (62)$$

while, for $n = 0$ we are allowed (See Appendix A 2)

$$R_{n=0, k}(r) = c_1 J_\nu(kr) + c_2 N_\nu(kr) \quad (0 \leq r \leq r_b), \quad (63)$$

From here on we set $c_2 = 0$, however we find no physical argument as to why this must necessarily be true^[8]. For the exterior solutions we use Hankel functions for later convenience, and find (for all n)

$$R_{n,k}(r) = H_\nu^{(2)}(kr_{\text{out}}) H_\nu^{(1)}(kr) - H_\nu^{(1)}(kr_{\text{out}}) H_\nu^{(2)}(kr) \quad (r_b \leq r \leq r_{\text{out}}), \quad (64)$$

[8] In fact, we must only ensure that the Hamiltonian is Hermitian and that the modes are normalizable; there is nothing inherently wrong with singular modes unless, of course, physical quantities diverge. The ambiguity in the value of c_2 represents an ignorance of what lies at the cone's tip; presumably it would be determined uniquely if the structural details of the tip were resolved.

where we have already imposed the Dirichlet condition at r_{out} . The spectrum of k are determined by the boundary conditions at r_b :

$$0 = \begin{cases} R_{n,k}(r_b) & \text{(Dirichlet),} \\ R'_{n,k}(r_b) & \text{(Neumann).} \end{cases} \quad (65)$$

2. Procedure for Calculation of Casimir Energy on the Cone

Contour Integral Representation of Sums

Again, we have no explicit expression for the $\{k\}$, and so we calculate (4) in part using the contour integral representation

$$\sum_{\{k\}} k^{1-2s+m} = -\frac{\cos \pi \left(\frac{m}{2} - s\right)}{\pi} \int_0^\infty dk k^{1-2s+m} \frac{\partial}{\partial k} \ln \Delta_n(ik) \quad (66)$$

where the contour has already been deformed. Lastly, we must specify the mode generating functions, which are derived analogously to the case of the horn (see Appendix B 4). We find these functions for both sides of r_b to effectively combine to give the log of the total generating function

$$\ln \Delta_n(ik) = \begin{cases} \ln [I_\nu(kr_b) K_\nu(kr_b)] & \text{(Dirichlet),} \\ \ln [I'_\nu(kr_b) K'_\nu(kr_b)] & \text{(Neumann).} \end{cases} \quad (67)$$

where any r_b -independent terms have been omitted as they play no role in the Casimir effect.

General Analysis of $E_0(s)$

We need to separate out the divergent parts from $E_0(s)$ so that they may be either analytically continued in s or explicitly absorbed through some renormalization(s). Because

the summand is even in n , we will have contributions to the energy of the form

$$E_0^{(n=0)} \propto \int_0^\infty dk k^{1-2s+m} \frac{\partial}{\partial k} \ln \Delta_0(ik) \quad (68)$$

and

$$E_0^{(n \neq 0)} \propto \sum_{n=1}^\infty \int_0^\infty dk k^{1-2s+m} \frac{\partial}{\partial k} \ln \Delta_n(ik) \quad (69)$$

Given (67), an analytic continuation of these expressions is impossible in its current form.

We want to decompose $E_0(s)$ into a sum of its asymptotic and finite part:

$$E_0(s) \equiv E_0^{\text{as}}(s) + E_0^{\text{fin}} \quad (70)$$

For $n = 0$ this simply means performing an expansion of $\ln \Delta_0(ik)$ in inverse powers of k . Following [23], we use the large k expansion to define

$$\tilde{\ln} [K_0(kr_b) I_0(kr_b)] \equiv \ln \left[\frac{1}{2kr_b} \right] + \sum_{j=1}^{m+1} \frac{A_j}{(kr_b)^j} \quad (\text{Dirichlet}) \quad (71)$$

$$\tilde{\ln} [K'_0(kr_b) I'_0(kr_b)] \equiv \ln \left[-\frac{1}{2kr_b} \right] + \sum_{j=1}^{m+1} \frac{B_j}{(kr_b)^j} \quad (\text{Neumann}) \quad (72)$$

where the first few coefficients are $A_2 = 1/8, A_4 = 13/64, B_2 = -3/8, B_4 = -27/64$ and $A_j = B_j = 0$ for all odd j . We thus capture all the divergences by taking

$$E_0^{\text{as}(n=0)} \propto \int_0^\infty dk k^{1-2s+m} \frac{\partial}{\partial k} \tilde{\ln} [K_0(kr_b) I_0(kr_b)] \quad (73)$$

for the Dirichlet case, and similarly for Neumann. For $n \neq 0$, we employ a uniform asymptotic expansion (as done for the horn) by first making the variable change

$$y \equiv \frac{k}{\nu} \quad (74)$$

therefore our sum/integral becomes

$$E_0^{(n \neq 0)} \propto \sum_{n=1}^\infty \nu^{1-2s+m} \int_0^\infty dy y^{1-2s+m} \frac{\partial}{\partial y} \ln \Delta_n(i\nu y) \quad (75)$$

From the uniform asymptotic behavior of the two modified Bessel functions (see e.g. [21]) we define the asymptotic part of the log of the generating function to be

$$\tilde{\ln} [K_\nu(\nu y r_b) I_\nu(\nu y r_b)] \equiv \ln \left[\frac{1}{2\nu} \frac{1}{\sqrt{y^2 r_b^2 + 1}} \right] + \sum_{j=1}^{m+2} \frac{f_j(y r_b)}{\nu^j} \quad (\text{Dirichlet}) \quad (76)$$

$$\tilde{\ln} [K'_\nu(\nu y r_b) I'_\nu(\nu y r_b)] \equiv \ln \left[-\frac{1}{2\nu} \frac{\sqrt{y^2 r_b^2 + 1}}{y^2 r_b^2} \right] + \sum_{j=1}^{m+2} \frac{h_j(y r_b)}{\nu^j} \quad (\text{Neumann}), \quad (77)$$

where the $f_j(z)$ and $h_j(z)$ are given in Appendix C. We therefore capture all the divergences of (75) by taking

$$E_0^{\text{as } (n \neq 0)} \propto \sum_{n=1}^{\infty} \nu^{1-2s+m} \int_0^{\infty} dy y^{1-2s+m} \frac{\partial}{\partial y} \tilde{\ln} [K_\nu(\nu y r_b) I_\nu(\nu y r_b)]. \quad (78)$$

for the Dirichlet case, and similarly for Neumann. In all cases, E_0^{fin} is obtained from the difference of $E_0(s)$ and $E_0^{\text{as}}(s)$. To recap, we have in total

$$E = E_{\text{ten}} + E_{\text{curv}} + E_0^{\text{as}}(s) + E_0^{\text{fin}} \quad (D = 2 + 1) \quad (79)$$

$$\rho = \rho_{\text{ten}} + \rho_{\text{curv}} + \rho_0^{\text{as}}(s) + \rho_0^{\text{fin}} + \rho_{0, \text{SM}} \quad (D = 5 + 1) \quad (80)$$

B. $D = 2 + 1$

Here there are no Minkowski dimensions, so $\mathbf{p} = 0$ and $m = 0$. From (4) and (66) we find

$$E_0(s) = -\frac{\mu^{2s}}{2\pi} \cos \pi s \left(\int_0^{\infty} dk k^{1-2s} \frac{\partial}{\partial k} \ln \Delta_0(ik) + 2 \sum_{n=1}^{\infty} \int_0^{\infty} dk k^{1-2s} \frac{\partial}{\partial k} \ln \Delta_n(ik) \right) \quad (81)$$

1. Dirichlet Condition

The $n = 0$ modes: In this case we isolate the divergent part as

$$E_0^{\text{as } (n=0)} = -\frac{\mu^{2s}}{2\pi} \cos \pi s \int_{\Lambda_{\text{IR}}}^{\infty} dk k^{1-2s} \frac{\partial}{\partial k} \tilde{\ln} [I_0(kr_b) K_0(kr_b)] \quad (82)$$

which vanishes after taking both $\Lambda_{\text{IR}} \rightarrow 0$ and $s \rightarrow 0$, the order being irrelevant. The finite piece is then found numerically (after integration by parts)

$$\begin{aligned} E_0^{\text{fin } (n=0)} &= +\frac{1}{2\pi} \int_0^{\infty} dk \left[\ln [I_0(kr_b) K_0(kr_b)] - \tilde{\ln} [I_0(kr_b) K_0(kr_b)] \right] \\ &\approx -\frac{1.4 \times 10^{-2}}{r_b} \end{aligned} \quad (83)$$

The $n \neq 0$ modes: Here we have (with $k = \nu y$)

$$E_0^{\text{as } (n \neq 0)} = -\frac{\mu^{2s}}{\pi} \cos \pi s \sum_{n=1}^{\infty} \nu^{1-2s} \int_0^{\infty} dy y^{1-2s} \frac{\partial}{\partial y} \tilde{\ln} [I_\nu(\nu y r_b) K_\nu(\nu y r_b)] \quad (84)$$

$$= \frac{1}{24(1-\delta)r_b} - \frac{(1-\delta)}{128r_b} \left(3 + \gamma + \frac{1}{2s} + \ln [\mu r_b (1-\delta)] \right) \quad (85)$$

The finite piece is

$$E_0^{\text{fin } (n \neq 0)} = +\frac{1}{\pi} \sum_{n=1}^{\infty} \int_0^{\infty} dk \left[\ln [I_\nu(kr_b) K_\nu(kr_b)] - \tilde{\ln}[I_\nu(kr_b) K_\nu(kr_b)] \right] \quad (86)$$

$$= \frac{\mathcal{N}(\delta)}{r_b} \quad (87)$$

where $\mathcal{N}(\delta)$ is a numerical coefficient; we find $\mathcal{N}(0) \approx 9.7 \times 10^{-4}$ (when the cone is opened fully) and that its magnitude decreases to zero^[9] monotonically as $\delta \rightarrow 1$ (in the limit the cone closes in on itself).

Summary: A $1/s$ pole remains whose existence we verify using a heat kernel analysis in Appendix E and, based on how this term scales, we identify h as the parameter that must be renormalized. Taking the total energy as the sum of the tension energy, the renormalized curvature, and the vacuum contributions we find

$$E(r_b) \approx 2\pi(1-\delta)r_b\sigma + \frac{2\pi(1-\delta)h_{\text{ren}}}{r_b} - \frac{1.3 \times 10^{-2}}{r_b} + \frac{1}{24} \frac{1}{(1-\delta)r_b} - \frac{(1-\delta)\ln\mu r_b}{128r_b} \quad (88)$$

where we have also absorbed finite quantum corrections in h_{ren} . The scale μ remains in the argument of the logarithm, as it must for it be unitless. This scale, however, is arbitrary and completely degenerate with the measured value of h_{ren} , and may be chosen to be anything convenient. Then, without loss of generality, we define μ as the scale at which $h_{\text{ren}} = 0$. The logarithmic term dominates in both the $r_b \rightarrow 0$ and $r_b \rightarrow \infty$ limits and, because of its overall minus sign, the energy has a global minimum (see Figure 8). Having $\sigma > 0$ simply steepens the potential, however it isn't required for stability.

Finally, as a check on our results, we set $\sigma = \delta = 0$, to recover the scalar Casimir energy of a 1-sphere with a Dirichlet boundary condition (e.g. [19, 24])

$$\mu^{-1} E_0(\mu^{-1}) \approx 6.8 \times 10^{-4} \quad (89)$$

[9] This is consistent with the fact that in this limit $\tilde{\ln}[\cdot]$ becomes a better approximation to $\ln[\cdot]$ since it is defined as an expansion in large ν .

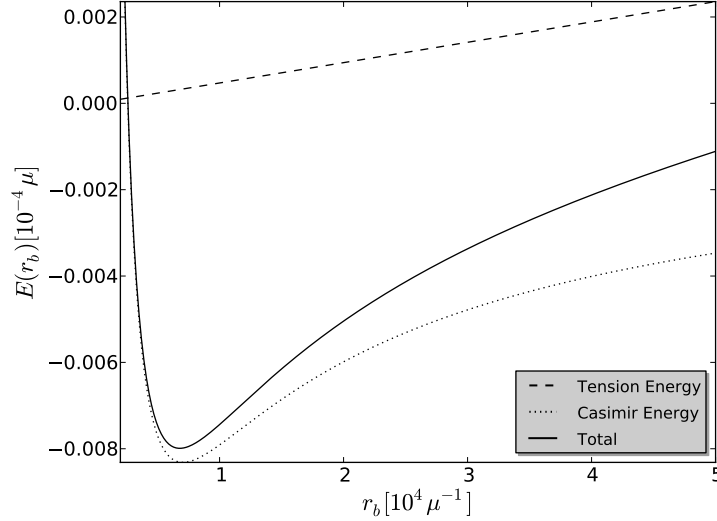


FIG. 8: For $D = 2 + 1$ with the Dirichlet boundary condition on ϕ , the total energy in units (μ) where $h_{\text{ren}} = 0$, as a function of the boundary position, r_b . For illustration, we have taken $\delta = 1/4$ and the brane tension, $\sigma = 10^{-12} [\mu^2]$.

2. Neumann Condition

Here we proceed as in the previous section, using (67). We find the total energy to be

$$E(r_b) \approx 2\pi (1 - \delta) r_b \sigma + \frac{2\pi (1 - \delta) h_{\text{ren}}}{r_b} - \frac{0.25}{r_b} - \frac{1}{24 (1 - \delta) r_b} - \frac{5 (1 - \delta)}{128 r_b} \ln \mu r_b \quad (90)$$

As in the Dirichlet case, the log term dominates in both limits of r_b , meaning there is again a global minimum^[10] in the potential (see Figure 9). As a check on our results, we set $\sigma = \delta = 0$, to recover the scalar Casimir energy of a 1-sphere with a Neumann boundary condition [19, 24]

$$\mu^{-1} E_0(\mu^{-1}) \approx -0.18 \quad (91)$$

[10] One may notice a large difference in scales between the Dirichlet and Neumann case, namely that the minima lie at around $10^4 \mu^{-1}$ and $10^{-4} \mu^{-1}$, respectively. This is traced back to the logarithmic behavior of the potential, therefore the minimum depends exponentially on $\mathcal{O}(1)$ numbers that are either > 0 or < 0 .

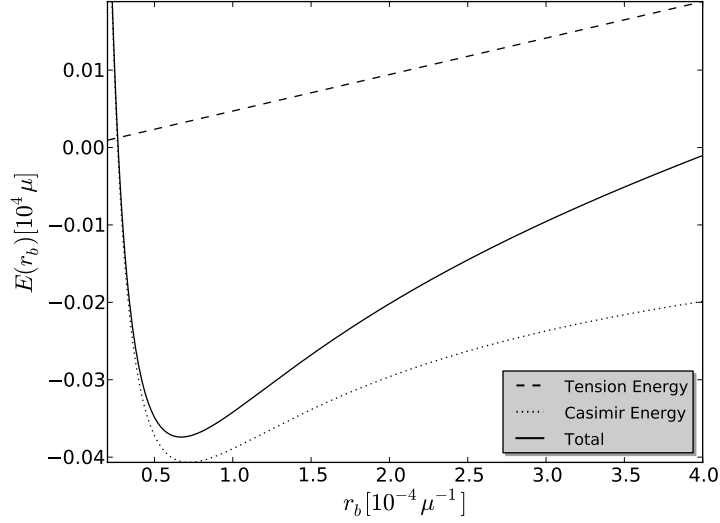


FIG. 9: For $D = 2 + 1$ with the Neumann boundary condition, the total energy in units (μ) where $h_{\text{ren}} = 0$, as a function of the boundary position, r_b . For illustration, we have taken $\delta = 1/4$ and the brane tension, $\sigma = 10^5 [\mu^2]$.

C. $D = 5 + 1$

Here, we treat the addition of three Minkowski spatial dimensions ($m = 3$) in the same manner as Section II C, regulating the size of the Minkowski spatial slice by compactifying these dimensions using a torus of fundamental side length, $V_M^{1/3}$. Using the same logic and the result (66) we find the effective 4D vacuum energy

$$\begin{aligned}
 \rho_0(s) &= \frac{\mu^{2s}}{16\pi^{5/2}} \frac{\Gamma(s-2)}{\Gamma(s-1/2)} \sin \pi s \sum_n \int_0^\infty dk k^{4-2s} \frac{\partial}{\partial k} \ln \Delta_n(ik) \\
 &= -\frac{\mu^{2s}}{64\pi^2} \left(1 + s \left(\frac{3}{2} - \gamma - \psi(-1/2) \right) \right) \times \\
 &\quad \left(\int_0^\infty dk k^{4-2s} \frac{\partial}{\partial k} \ln \Delta_0(ik) + 2 \sum_{n=1}^\infty \int_0^\infty dk k^{4-2s} \frac{\partial}{\partial k} \ln \Delta_n(ik) \right) \quad (92)
 \end{aligned}$$

1. *Dirichlet Condition*

The $n = 0$ modes: Here we define the analytic part as

$$\begin{aligned}\rho_0^{\text{as } (n=0)} &= -\frac{\mu^{2s}}{64\pi^2} \left(1 + s \left(\frac{3}{2} - \gamma - \psi(-1/2) \right) \right) \int_{\Lambda_{\text{IR}}}^{\infty} dk k^{4-2s} \frac{\partial}{\partial k} \tilde{\ln} [I_0(kr_b) K_0(kr_b)] \\ &= \frac{13}{2048\pi^2 r_b^4} \left(\frac{1}{s} + 2 \ln \mu r_b + \frac{15}{26} - \gamma - \psi(-1/2) \right)\end{aligned}\quad (93)$$

where in the second line we have chosen^[11] $\Lambda_{\text{IR}} = r_b^{-1}$. The finite piece is then

$$\begin{aligned}\rho_0^{\text{fin } (n=0)} &= -\frac{1}{64\pi^2} \left(\int_0^{\Lambda_{\text{IR}}} dk k^4 \frac{\partial}{\partial k} \ln [I_0(kr_b) K_0(kr_b)] \right. \\ &\quad \left. + \int_{\Lambda_{\text{IR}}}^{\infty} dk k^4 \frac{\partial}{\partial k} \left[\ln [I_0(kr_b) K_0(kr_b)] - \tilde{\ln} [I_0(kr_b) K_0(kr_b)] \right] \right) \\ &\approx -5.4 \times 10^{-4} \times \frac{1}{r_b^4}\end{aligned}\quad (94)$$

The $n \neq 0$ modes: Here, with $k = \nu y$ we have

$$\begin{aligned}\rho_0^{\text{as } (n \neq 0)} &= -\frac{\mu^{2s}}{32\pi^2} \left(1 + s \left(\frac{3}{2} - \gamma - \psi(-1/2) \right) \right) \sum_{n=1}^{\infty} \nu^{4-2s} \int_0^{\infty} dy y^{4-2s} \frac{\partial}{\partial y} \tilde{\ln} [I_\nu(\nu y r_b) K_\nu(\nu y r_b)] \\ &= \frac{13}{2048\pi^2 r_b^4} \left(\gamma - \frac{1}{s} - 2 \ln [2\pi(1-\delta)r_b\mu] + \psi(-1/2) \right) + \frac{199}{8192\pi^2 r_b^4} \\ &\quad - \frac{7\zeta'(-2)}{64\pi^2 (1-\delta)^2 r_b^4} + \frac{\zeta'(-4)}{32\pi^2 (1-\delta)^4 r_b^4}\end{aligned}\quad (95)$$

Leaving us with a finite part given by

$$\rho_0^{\text{fin } (n \neq 0)} = +\frac{1}{8\pi^2} \sum_{n=1}^{\infty} \int_0^{\infty} dk k^3 \left[\ln [I_\nu(kr_b) K_\nu(kr_b)] - \tilde{\ln} [I_\nu(kr_b) K_\nu(kr_b)] \right] \quad (96)$$

$$\approx \mathcal{N}(\delta) \times \frac{1}{r_b^4} \quad (97)$$

where $\mathcal{N}(\delta)$ is a numerical coefficient. It is about -2.8×10^{-4} for $\delta = 0$ and its magnitude decreases to zero monotonically as δ increases towards 1.

[11] In the $D = 2 + 1$ cases we were able to simply analytically continue $\Lambda_{\text{IR}} \rightarrow 0$. Here we must choose it to be finite (but arbitrary) and $\Lambda_{\text{IR}} = r_b^{-1}$ is convenient for displaying our results. To be clear, the sum $\rho_0^{(n=0)} = \rho_0^{\text{as } (n=0)} + \rho_0^{\text{fin } (n=0)}$ is independent of Λ_{IR} in the $s \rightarrow 0$ limit.

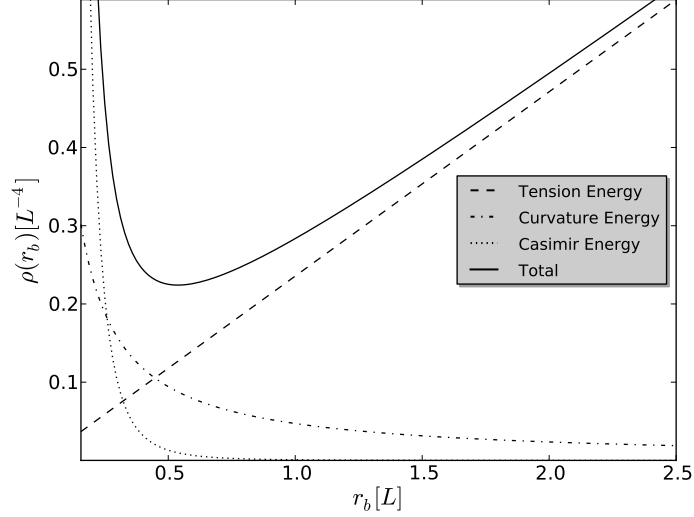


FIG. 10: For the $D = 5 + 1$ Dirichlet condition, the total 4D energy density vs. brane position using an arbitrary unit of length, L , as a function of the boundary position, r_b . For illustration, we have taken $\delta = 1/4$, $\sigma = 0.05 [L^{-5}]$, $h = 0.01 [L^{-3}]$, $\kappa_{SM} = 0$.

Summary: Taking the total energy as the sum of the tension, renormalized curvature, and vacuum energy contributions, we have

$$\begin{aligned} \rho(r_b) \approx & 2\pi(1-\delta)r_b\sigma + \frac{2\pi(1-\delta)h_{\text{ren}}}{r_b} + \frac{229}{8192\pi^2r_b^4} - \frac{13\ln[2\pi(1-\delta)]}{1024\pi^2r_b^4} \\ & - \frac{7\zeta'(-2)}{64\pi^2(1-\delta)^2r_b^4} + \frac{1}{16\pi^4(1-\delta)^4r_b^4} \left(\frac{1}{2}\pi^2\zeta'(-4) + \kappa_{SM} \right) \end{aligned} \quad (98)$$

where $1/2\pi^2\zeta'(-4) \approx 0.04$. Here the $1/s$ poles have canceled when the $n = 0$ and $n \neq 0$ modes were added together. As $r_b \rightarrow 0$ the energy is unbounded from above for all δ , neglecting κ_{SM} . Therefore, if a positive brane tension exists the energy has a stable minimum. Since the cone has no intrinsic length scale we choose use an arbitrary scale, L , as a reference with which to plot our results in Fig 10. Interestingly, even in the absence of the Casimir effects of the bulk scalar, a stable minimum is achieved if we take both h and σ to be positive, a physically reasonable assumption.

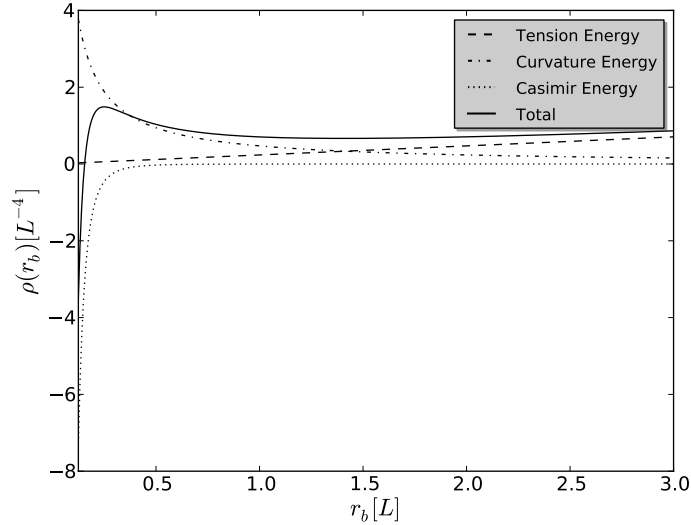


FIG. 11: For the $D = 5+1$ Neumann condition, the total 4D energy density using an arbitrary unit of length, L , as a function of the boundary position, r_b . For illustration, we have chosen $\delta = 1/4$, $\sigma = 0.05 [L^{-5}]$, $h = 0.1 [L^{-3}]$, $\kappa_{SM} = 0$.

2. Neumann Condition

Summary: Here we proceed as in the previous section, only using (67). The total 4D energy density is found to be

$$\begin{aligned} \rho(r_b) \approx & 2\pi(1-\delta)r_b\sigma + \frac{2\pi(1-\delta)h}{r_b} - \frac{7309}{122880\pi^2r_b^4} + \frac{27\ln[2\pi(1-\delta)]}{1024\pi^2r_b^4} \\ & + \frac{13\zeta'(-2)}{64\pi^2(1-\delta)^2r_b^4} + \frac{1}{16\pi^4(1-\delta)^4r_b^4} \left(-\frac{1}{2}\pi^2\zeta'(-4) + \kappa_{SM} \right) \end{aligned} \quad (99)$$

Here the energy is unbounded from below as $r_b \rightarrow 0$ for all δ , neglecting κ_{SM} . A global minimum apparently doesn't exist when κ_{SM} is negligible, however because of the different scaling behavior of each contribution to the potential, a local minimum is possible for large enough h . We have plotted this case in Fig 11, again using a reference scale, L .

IV. CONCLUSIONS

In this work we have generalized the analysis in [17], demonstrating that a single brane embedded in a bulk spacetime can be localized and stabilized using various contributions to

its effective potential, specifically exploiting the non-trivial geometry and/or topology of the bulk manifold. We have focused on the hyperbolic horn and Euclidean cone geometries as they have features that are generic to more general manifolds yet still allow our calculations to be tractable. We have considered a brane wrapped around both manifolds, calculating the energy due to tension and extrinsic curvature (i.e. due to local brane geometry) and also due to the Casimir energy of a bulk scalar (a global effect). Both types of contributions are generally regional in nature, most sensitive to a finite region within the spatial manifold. The spaces considered here might be taken seriously for model building, as an approximation to capture the *regional* features of a more generic manifold, or perhaps simply as a toy example of how various forces can be used to stabilize branes embedded within non-trivial manifolds.

We have considered both Dirichlet and Neumann boundary conditions for the bulk scalar at the location of the brane in both dimensions $D = 2 + 1$ and $D = 5 + 1$, i.e. without and with 3 Minkowski dimensions, respectively. Though we don't appear to live in $D = 2 + 1$, those systems are interesting as they illustrate how the Casimir effect changes its behavior with the number of dimensions, perhaps most notably how the explicit presence of poles in the energy depend on whether D is even or odd. In Table I we summarize our results on the type of minima found for each brane potential, assuming the geometric energies are positive ($\sigma, h > 0$) and that the Casimir energy of Standard Model fields in $D = 5 + 1$ are negligible ($\kappa_{SM} \ll 1$).

Case	$D = 2 + 1$		$D = 5 + 1$	
	Dirichlet	Neumann	Dirichlet	Neumann
Horn	global	none	global	none
Cone	global	global	global	local

TABLE I: Summary of brane potentials, indicating whether a global, local or no minimum is possible, assuming κ_{SM} is negligible.

Interestingly, for the cone we have demonstrated that a potential minimum is possible in the absence of Casimir energy; the competition between purely geometrical effects (tension and elastic energy) are sufficient to stabilize the brane. Physically, this is the result of tension energy being minimized by shrinking the volume of the brane, while the elastic energy is minimized by flattening it. On the cone, these two effects come in with markedly

different dependences on the brane position, therefore an extremum is possible. For the horn, however, these energies have the same brane position dependence and therefore the same cannot be said on that geometry.

Because the geometries we have chosen still retain a scaling symmetry, there are only two “special” places on each manifold, i.e. $(-\infty, +\infty)$ or $(0, +\infty)$ on the horn and cone, respectively. As a result, all of the energy contributions behave monotonically with brane position and so are either minimized in the limit that the brane approaches one or the other. For this reason, we have found a necessary competition between at least two of them in order to achieve a stable minimum.

In fact, this is an especially important point in the case that we live on a 3-brane. In those scenarios the brane may be visualized (suppressing the 3 Minkowski dimensions) as a point embedded in the bulk, having only trivial geometric properties that don’t result in position-dependent forces. With (apparently) only the Casimir effect remaining, there is likely no global minimum^[12] for the brane potential on either the horn or the cone in this case and such a brane could only be driven to one of the extremes of the manifold. However this will not generically be the case; manifolds with sufficient symmetry violation will have many “special” places – places where one or many of the energies are extremized, especially Casimir.

Finally, we note that the discussion of regional effects of bulk manifolds is not limited to braneworld scenarios, alone. Perhaps the most interesting (and generic) feature of non-trivial regional properties of extra-dimensional manifolds is the inhomogeneity of field modes of the bulk.

We would like to thank Ling-yi Huang, Harsh Mathur and Claudia de Rham for many useful discussions. This work is supported by grants from the U.S. Department of Energy and Department of Education.

[12] However a local minimum may be possible by the competition of Casimir energies from several fields of varying mass and spin (see e.g. [15]).

-
- [1] N. Arkani-Hamed, S. Dimopoulos, and G. Dvali *Phys.Lett.* **B429** (1998) 263–272, [hep-ph/9803315].
- [2] I. Antoniadis, N. Arkani-Hamed, S. Dimopoulos, and G. Dvali *Phys.Lett.* **B436** (1998) 257–263, [hep-ph/9804398].
- [3] L. Randall and R. Sundrum *Phys.Rev.Lett.* **83** (1999) 3370–3373, [hep-ph/9905221].
- [4] N. Arkani-Hamed and M. Schmaltz *Phys.Rev.* **D61** (2000) 033005, [hep-ph/9903417].
- [5] G. Dvali, G. Gabadadze, and M. Porrati *Phys.Lett.* **B485** (2000) 208–214, [hep-th/0005016].
- [6] G. Dvali, S. Hofmann, and J. Khoury *Phys.Rev.* **D76** (2007) 084006, [hep-th/0703027].
- [7] C. de Rham, G. Dvali, S. Hofmann, J. Khoury, O. Pujolas, M. Redi, and A. Tolley *Phys.Rev.Lett.* **100** (2008) 251603, [arXiv:0711.2072].
- [8] N. Kaloper, J. March-Russell, G. D. Starkman, and M. Trodden *Phys.Rev.Lett.* **85** (2000) 928–931, [hep-ph/0002001].
- [9] D. Orlando and S. Park *JHEP* **1008** (2010) 006, [arXiv:1006.1901].
- [10] D. Kapner, T. Cook, E. Adelberger, J. Gundlach, B. R. Heckel, et al. *Phys.Rev.Lett.* **98** (2007) 021101, [hep-ph/0611184].
- [11] W. D. Goldberger and M. B. Wise *Phys.Rev.Lett.* **83** (1999) 4922–4925, [hep-ph/9907447].
- [12] H. Casimir *Indag.Math.* **10** (1948) 261–263.
- [13] J. Garriga, O. Pujolas, and T. Tanaka *Nucl.Phys.* **B605** (2001) 192–214, [hep-th/0004109].
- [14] E. Ponton and E. Poppitz *JHEP* **0106** (2001) 019, [hep-ph/0105021].
- [15] B. R. Greene and J. Levin *JHEP* **0711** (2007) 096, [arXiv:0707.1062].
- [16] E. Elizalde, S. Nojiri, S. D. Odintsov, and S. Ogushi *Phys.Rev.* **D67** (2003) 063515, [hep-th/0209242].
- [17] D. M. Jacobs, G. D. Starkman, and A. J. Tolley arXiv:1205.1528.
- [18] T. Appelquist, H. Cheng, and B. A. Dobrescu *Phys.Rev.* **D64** (2001) 035002, [hep-ph/0012100].
- [19] M. Bordag, G. Klimchitskaya, U. Mohideen, and V. Mostepanenko, *Advances in the Casimir*

- effect*. Oxford, 2009.
- [20] D. Fursaev and D. Vassilevich, *Operators, geometry and quanta*. Springer, 2011. ISBN: 978-94-007-0204-2.
- [21] M. Abramowitz and I. A. Stegun, *Handbook of Mathematical Functions*. Dover, New York, 1964.
- [22] S. Blau, M. Visser, and A. Wipf *Nucl.Phys.* **B310** (1988) 163, [[arXiv:0906.2817](#)].
- [23] G. Arfken and H. Weber, *Mathematical Methods for Physicists, 6th ed.* Elsevier, 2005.
- [24] S. Leseduarte and A. Romeo *Annals Phys.* **250** (1996) 448–484, [[hep-th/9605022](#)].
- [25] J. Jackson, *Classical Electrodynamics*. Wiley, 3rd ed., 1998.
- [26] W. H. Press, S. A. Teukolsky, W. T. Vetterling, and B. P. Flannery, *Numerical Recipes*. Cambridge University Press, New York, NY, USA, 3 ed., 2007.
- [27] E. Elizalde *J.Phys.* **A41** (2008) 304040, [[arXiv:0712.1346](#)].
- [28] D. Vassilevich *Phys.Rept.* **388** (2003) 279–360, [[hep-th/0306138](#)].

Appendix A: Details of Mode Solutions

1. Hyperbolic Horn

a. $n \neq 0$

From (10) we have

$$Z''_{n,k}(z) - Z'_{n,k}(z) + \left(k^2 + \frac{1}{4} - n^2 e^{2z}\right) Z_{n,k}(z) = 0 \quad (\text{A1})$$

where we have defined k by $\omega \equiv \sqrt{p^2 + k^2 + \frac{1}{4}}$. With the substitutions $\rho = |n|e^z$, $Z(\rho) \equiv \rho^{1/2}T(\rho)$, and $k \equiv -i\nu$ we obtain

$$T_{\rho\rho} + \frac{1}{\rho}T_{\rho} - \left(\frac{\nu^2}{\rho^2} + 1\right)T = 0 \quad (\text{A2})$$

This familiar equation is the modified Bessel equation, whose two linearly independent solutions are the modified Bessel functions of the first and second kind, $I_{\nu}(\rho)$ and $K_{\nu}(\rho)$, respectively (see, e.g. [25]). Returning to the original variables, we have

$$Z_{n,k}(z) = e^{z/2} (c_1 I_{ik}(|n|e^z) + c_2 K_{ik}(|n|e^z)), \quad (z \geq z_b) \quad (\text{A3})$$

In this region, the Klein-Gordon norm tells us

$$\int_{z_b}^{\infty} dz e^{-z} Z_i(z)^* Z_j(z) = \delta_{ij} \quad (\text{A4})$$

Asymptotically, $I_{\mu}(x) \sim |x|^{-1/2}e^x$ as $x \rightarrow \infty$, regardless of μ , making the solution non-normalizable unless we take $c_1 = 0$. Furthermore, the modified Bessel functions $I_{\mu}(x), K_{\mu}(x)$ are monotonic for $\mu \in \mathbb{R}$, meaning neither $K_{ik}(|n|e^z)$ nor its derivative vanish for finite z . As the $k \leftrightarrow -k$ solutions are linearly related, this indicates that only real, $k > 0$ are permissible.

In fact, $I_{\nu}(\rho)$ and $I_{-\nu}(\rho)$ also form a set of linearly independent solutions to (A2), so long as both $\nu \notin \mathbb{Z}$ and $i\nu \notin \mathbb{Z}$ [13]. For later convenience, we use

$$Z_{n,k}(z) = e^{z/2} (c_1 I_{ik}(|n|e^z) + c_2 I_{-ik}(|n|e^z)), \quad (z_L \leq z \leq z_b) \quad (\text{A5})$$

where the two boundary conditions at z_L and z_b plus the normalization condition completely determine c_1, c_2 and the allowable k .

[13] One may worry about the possibility of $k \in \mathbb{Z}$, however those cases are contrived; the set of model parameters for which this is true form a set of measure zero.

For the region $z_L \leq z \leq z_b$ the conditions necessary to have a zero at z_L tell us (up to a normalization factor)

$$Z_{n,k}(z) = e^{z/2} (I_{-ik}(|n|e^{z_L})I_{ik}(|n|e^z) - I_{ik}(|n|e^{z_L})I_{-ik}(|n|e^z)) \quad (\text{A6})$$

In the case of Dirichlet boundary condition, the zero at z_b then implies the relation

$$\frac{I_{ik}(|n|e^{z_b})}{I_{-ik}(|n|e^{z_b})} = \frac{I_{ik}(|n|e^{z_L})}{I_{-ik}(|n|e^{z_L})}. \quad (\text{A7})$$

and there is a similar relation for the Neumann case. When $ik \in \mathbb{R}$, the monotonicity of the modified Bessel function implies this equation may only be satisfied in the trivial case, $z_L = z_b$. All things considered, this means only real, $k > 0$ are allowed. In summary,

$$\begin{aligned} Z(z) &= e^{z/2} [I_{-ik}(|n|e^{z_L})I_{ik}(|n|e^z) - I_{ik}(|n|e^{z_L})I_{-ik}(|n|e^z)] & (z_L \leq z \leq z_b) \\ &= e^{z/2} K_{ik}(|n|e^z) & (z_b \leq z) \end{aligned} \quad (\text{A8})$$

b. $n = 0$

From (10) we have

$$Z''(z) - Z'(z) + \left(k^2 + \frac{1}{4}\right) Z(z) = 0 \quad (\text{A9})$$

The solutions are

$$Z(z) = e^{z/2} (c_1 e^{ikz} + c_2 e^{-ikz}) \quad (\text{A10})$$

To obviate having to delta function-normalize the modes in the region $z \geq z_b$, we truncate the space at some $z_R > z_b$, taking the limit $z_R \rightarrow \infty$ at the end of the calculation. This quantizes the modes in this region as well. After imposing zero at z_L and z_R the solutions are

$$Z_{0,k} = e^{z/2} \sin k(z - z_L) \quad (z_L \leq z \leq z_b) \quad (\text{A11})$$

$$= e^{z/2} \sin k(z - z_R) \quad (z_b \leq z \leq z_R) \quad (\text{A12})$$

Requiring either a Dirichlet or Neumann boundary condition in each region implies real, $k > 0$.

2. Euclidean Cone

Consider the interior solutions

$$R_{n,k}(r) = c_1 J_\nu(kr) + c_2 N_\nu(kr) \quad (0 \leq r \leq r_b), \quad (\text{A13})$$

for arbitrary n . Normalizability would tell us

$$\int_0^{r_b} dr r R_{n,k}(r)^2 = 1 \quad (\text{A14})$$

If $c_2 \neq 0$, the most dangerous part of this integral near $r = 0$ is

$$\int_0^{\epsilon} dr r N_\nu(kr)^2 \propto \int_0^{\epsilon} dr r r^{-2\nu}, \quad (\nu \neq 0) \quad (\text{A15})$$

$$\propto \int_0^{\epsilon} dr r (\ln p)^2, \quad (\nu = 0) \quad (\text{A16})$$

The first integral diverges because $\nu \geq 1$, while the second one converges. Therefore, on the basis of normalizability, $c_2 \neq 0$ is possible only for $\nu = 0$ ($n = 0$).

Appendix B: Calculating $E_0(s)$ via Contour Integrals

1. General Procedure

We will ensure $\Delta_n(k)$ to be a meromorphic function, having only simple zeros at the location of the k 's in the spectrum. Near the i th zero, the derivative of its logarithm produces the pole $(k - k_i)^{-1}$, plus other finite terms so that, by the Cauchy residue theorem, we have the relation

$$\sum_{\{k\}} (k^2 + \Lambda^2)^{\frac{m+1}{2}-s} = \frac{1}{2\pi i} \oint_{\gamma} dk (k^2 + \Lambda^2)^{\frac{m+1}{2}-s} \frac{\partial}{\partial k} \ln \Delta_n(k) \quad (\text{B1})$$

The beauty of this technique is that only the eigenfunctions need to be understood analytically.

Assuming no other poles/zeros in the $\text{Re } k > 0$ plane exist, the contour may be deformed (see Figure 12) by rotating counter-clockwise ($k \rightarrow e^{i\pi/2}k$) the upper contour, γ_1 , while the lower contour, γ_2 , is rotated clockwise ($k \rightarrow e^{-i\pi/2}k$). Thus the contour goes along the imaginary axis from $i\infty$ to $-i\infty$, discarding the rest of the boundary at $|k| \rightarrow \infty$. (This is

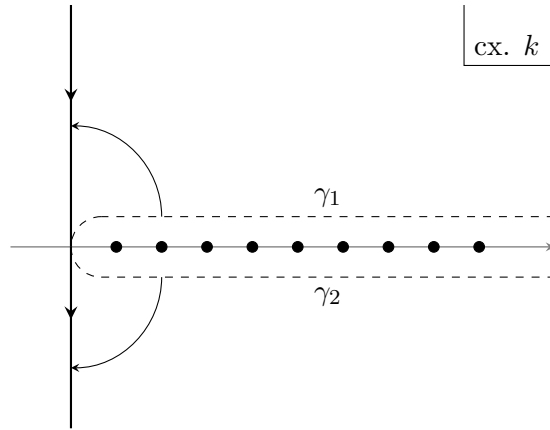


FIG. 12: Deformed contour.

legitimate so long as s is large enough; at the end of the calculation we analytically continue to $s = 0$). Care must be taken here as the function $(k^2 + \Lambda^2)^{\frac{m+1}{2}-s}$ is multivalued and has a branch point at $k = \pm\Lambda$. Explicitly, one finds

$$\begin{aligned}
& \frac{1}{2\pi i} \oint_{\gamma} dk (k^2 + \Lambda^2)^{\frac{m+1}{2}-s} \frac{\partial}{\partial k} \ln \Delta_n(k) \\
&= \frac{1}{2\pi i} \left(\int_{i\infty}^0 dk (k^2 + \Lambda^2)^{\frac{m+1}{2}-s} \frac{\partial}{\partial k} \ln \Delta_n(k) + \int_0^{-i\infty} dk (k^2 + \Lambda^2)^{\frac{m+1}{2}-s} \frac{\partial}{\partial k} \ln \Delta_n(k) \right) \\
&= \frac{1}{2\pi i} \int_0^{\infty} dk \left[(e^{-i\pi} k^2 + \Lambda^2)^{\frac{m+1}{2}-s} - (e^{i\pi} k^2 + \Lambda^2)^{\frac{m+1}{2}-s} \right] \frac{\partial}{\partial k} \ln \Delta_n(ik) \\
&= -\frac{\cos \pi \left(\frac{m}{2} - s \right)}{\pi} \int_{\Lambda}^{\infty} dk (k^2 - \Lambda^2)^{\frac{m+1}{2}-s} \frac{\partial}{\partial k} \ln \Delta_n(ik) \tag{B2}
\end{aligned}$$

where we have assumed that the chosen generating functions satisfy

$$\frac{\partial}{\partial k} \ln \Delta_n(ik) = \frac{\partial}{\partial k} \ln \Delta_n(-ik) \tag{B3}$$

Below we shall give a brief derivation of the mode-generating functions for both the horn and cone geometries with the Dirichlet boundary condition. The extension to the Neumann condition is straightforward.

2. Horn Generating Functions (Dirichlet, $n \neq 0$)

Here we need to calculate

$$\frac{1}{2\pi i} \oint_{\gamma} dk \left(k^2 + \frac{1}{4} \right)^{\frac{m+1}{2}-s} \frac{\partial}{\partial k} \ln \Delta_n(k) \tag{B4}$$

Considering (12) we choose the generating functions

$$\Delta_n(k) = \frac{1}{k} (I_{ik}(|n|e^{z_L}) I_{-ik}(|n|e^{z_b}) - I_{-ik}(|n|e^{z_L}) I_{ik}(|n|e^{z_b})), \quad (z_L \leq z \leq z_b) \quad (\text{B5})$$

$$\Delta_n(k) = K_{ik}(|n|e^{z_b}), \quad (z_b \leq z) \quad (\text{B6})$$

It will be of no consequence to the actual calculation^[14] but technically we had to explicitly include a factor of k^{-1} in (B5) to avoid counting the zero mode in the spectrum (at small k the term in parenthesis is proportional to k). As (B5) stands it is not useful, because we must still perform the limit $z_L \rightarrow -\infty$. Because of the asymptotic behavior $I_\mu(x) \sim (x/2)^\mu$ as $x \rightarrow 0$, in the limit of $z_L \rightarrow -\infty$ the surviving z_b -dependent terms of (B5) are

$$I_{-ik}(|n|e^{z_b}), \quad \text{on } \gamma_1 (\text{Re } k > 0) \quad (\text{B7})$$

$$I_{ik}(|n|e^{z_b}), \quad \text{on } \gamma_2 (\text{Re } k < 0) \quad (\text{B8})$$

When the contour is deformed, these two terms are equal and proportional to $I_k(|n|e^{z_b})$. Thus we effectively have

$$\Delta_n(ik) = I_k(|n|e^{z_b}), \quad (z_L \leq z \leq z_b) \quad (\text{B9})$$

$$\Delta_n(ik) = K_k(|n|e^{z_b}), \quad (z_b \leq z) \quad (\text{B10})$$

Since the energy of each region is simply be added (as the energies of two volumes sitting adjacent to each other), the two generating functions combine to give

$$\begin{aligned} & \frac{1}{2\pi i} \oint_\gamma dk \left(k^2 + \frac{1}{4} \right)^{\frac{m+1}{2}-s} \frac{\partial}{\partial k} \ln \Delta_n(k) \\ &= -\frac{\cos \pi \left(\frac{m}{2} - s \right)}{\pi} \int_{1/2}^\infty dk \left(k^2 - \frac{1}{4} \right)^{\frac{(m+1)}{2}-s} \frac{\partial}{\partial k} \ln [I_k(|n|e^{z_b}) K_k(|n|e^{z_b})] \quad (\text{B11}) \end{aligned}$$

3. Horn Generating Functions (Dirichlet, $n = 0$)

Here we will show that the sum over the k -spectrum is z_b -independent, and can therefore be ignored in the calculation of the Casimir energy. Before rotating the contour, we have

[14] Since a logarithm is taken of the generating function, if we multiply it by any analytic function of k this only contributes an additive (though possibly infinite) constant to E_0 , however this has no bearing on the Casimir force as it is z_b -independent.

an integral of the form

$$\frac{1}{2\pi i} \oint_{\gamma} dk \left(k^2 + \frac{1}{4} \right)^{\frac{(m+1)-s}{2}} \frac{\partial}{\partial k} \ln \Delta_0(k) \quad (\text{B12})$$

We break up the regions and, considering (A11), choose the generating functions to be

$$\begin{aligned} \Delta_0(k) &= \frac{1}{k} \left(e^{ik(z_b - z_L)} - e^{-ik(z_b - z_L)} \right) & (z_L \leq z \leq z_b) \\ \Delta_0(k) &= \frac{1}{k} \left(e^{ik(z_R - z_b)} - e^{-ik(z_R - z_b)} \right) & (z_b \leq z \leq z_R) \end{aligned} \quad (\text{B13})$$

First we consider the $z_L \leq z \leq z_b$ region, and take the limit $z_L \rightarrow -\infty$. On γ_1 ($\text{Im } k > 0$), $\Delta_0(k) \rightarrow e^{-ik(z_b - z_L)} k^{-1}$. On γ_2 ($\text{Im } k < 0$), $\Delta_0(k) \rightarrow e^{ik(z_b - z_L)} k^{-1}$. The same procedure may be performed for the $z_b \leq z \leq z_R$ region, taking $z_R \rightarrow \infty$. After the contour rotation, the effective generating functions for the left and right regions become $e^{k(z_b - z_L)}$ and $e^{k(z_R - z_b)}$, respectively. Thus, because of the logarithm, when the regions are combined the z_b -dependence vanishes and so these modes are irrelevant for the Casimir effect, as claimed.

4. Cone Generating Functions

Considering (62) and (64), we choose the generating functions

$$\Delta_n(k) = k^{-\nu} J_{\nu}(kr_b) \quad (0 \leq r \leq r_b) \quad (\text{B14})$$

$$\Delta_n(k) = (H_{\nu}^{(2)}(kr_{\text{out}}) H_{\nu}^{(1)}(kr_b) - H_{\nu}^{(1)}(kr_{\text{out}}) H_{\nu}^{(2)}(kr_b)) \quad (r_b \leq r \leq r_{\text{out}}) \quad (\text{B15})$$

The factor of $k^{-\nu}$ in the top line is so that the zero mode is not technically counted (at small k the term in parenthesis is proportional to k^{ν}). As it stands (B15) is not useful because we must still perform the limit $r_{\text{out}} \rightarrow \infty$. Because of the asymptotic behavior

$$\lim_{x \rightarrow \infty} H_{\nu}^{(1,2)}(x) \sim \sqrt{\frac{2}{\pi x}} e^{\pm i(x - \nu\pi/2 - \pi/4)}, \quad (\text{B16})$$

in the limit of $r_{\text{out}} \rightarrow \infty$ the surviving terms of (B15) are

$$H_{\nu}^{(2)}(kr_{\text{out}}) H_{\nu}^{(1)}(kr_b), \quad \text{on } \gamma_1 \text{ (Re } k > 0) \quad (\text{B17})$$

$$H_{\nu}^{(1)}(kr_{\text{out}}) H_{\nu}^{(2)}(kr_b), \quad \text{on } \gamma_2 \text{ (Re } k < 0) \quad (\text{B18})$$

When the contour is deformed, these two terms are both proportional to $I_\nu(kr_b)$, thus we effectively have

$$\Delta_n(ik) = I_\nu(kr_b) \quad (0 \leq r \leq r_b) \quad (\text{B19})$$

$$\Delta_n(ik) = K_\nu(kr_b) \quad (r_b \leq r \leq r_{\text{out}}) \quad (\text{B20})$$

Summing over the spectrum from each region we find

$$\frac{1}{2\pi i} \oint_\gamma dk k^{1-2s+m} \frac{\partial}{\partial k} \ln \Delta_n(k) = -\frac{\cos \pi \left(\frac{m}{2} - s\right)}{\pi} \int_{1/2}^\infty dk k^{1-2s+m} \frac{\partial}{\partial k} \ln [I_\nu(kr_b) K_\nu(kr_b)] \quad (\text{B21})$$

Appendix C: Bessel Function Asymptotics

Using the uniform asymptotic expansion of the modified Bessel functions (see e.g.[21]), one may show for the Dirichlet boundary conditions

$$\ln [I_\nu(\nu z) K_\nu(\nu z)] \sim \ln \left[\frac{1}{2\nu} \frac{1}{\sqrt{z^2 + 1}} \right] + \sum_{j=1}^\infty \frac{f_j(z)}{\nu^j} \quad (\text{C1})$$

where the first few non-zero $f_j(z)$ are

$$f_2(z) = \frac{(-4 + z^2)z^2}{8(1 + z^2)^3} \quad (\text{C2})$$

$$f_4(z) = \frac{(-32 + 288z^2 - 232z^4 + 13z^6)z^2}{64(1 + z^2)^6} \quad (\text{C3})$$

$$f_6(z) = \frac{(-48 + 2580z^2 - 14884z^4 + 17493z^6 - 4242z^8 + 103z^{10})z^2}{96(1 + z^2)^9} \quad (\text{C4})$$

For the Neumann condition on the horn one finds

$$\begin{aligned} & \ln \left[\frac{1}{4} I_\nu(\nu z) K_\nu(\nu z) + \frac{1}{2} \nu z (I_\nu(\nu z) K'_\nu(\nu z) + I'_\nu(\nu z) K_\nu(\nu z)) + (\nu z)^2 I'_\nu(\nu z) K'_\nu(\nu z) \right] \\ & \sim \ln \left[-\frac{\nu}{2} \sqrt{z^2 + 1} \right] + \sum_{j=1}^\infty \frac{g_j(z)}{\nu^j} \end{aligned} \quad (\text{C5})$$

where the first few non-zero $g_j(z)$ are

$$g_2(z) = \frac{-2 + 4z^2 - z^4}{8(1 + z^2)^3} \quad (\text{C6})$$

$$g_4(z) = \frac{-2 + 80z^2 - 372z^4 + 240z^6 - 13z^8}{64(1 + z^2)^6} \quad (\text{C7})$$

$$g_6(z) = \frac{-1 + 276z^2 - 8031z^4 + 36182z^6 - 37659z^8 + 8628z^{10} - 209z^{12}}{192(1 + z^2)^9} \quad (\text{C8})$$

Finally, for the Neumann condition on the cone, one may show

$$\ln [K'_\nu(\nu z) I'_\nu(\nu z)] \sim \ln \left[-\frac{1}{2\nu} \frac{\sqrt{z^2+1}}{z^2} \right] + \sum_{j=1}^{\infty} \frac{h_j(z)}{\nu^j} \quad (\text{C9})$$

where the first few non-zero $h_j(z)$ are

$$h_2(z) = \frac{(4-3z^2)z^2}{8(1+z^2)^3} \quad (\text{C10})$$

$$h_4(z) = \frac{(32-320z^2+328z^4-27z^6)z^2}{64(1+z^2)^6} \quad (\text{C11})$$

$$h_6(z) = \frac{(48-2652z^2+16180z^4-20799z^6+5652z^8-162z^{10})z^2}{96(1+z^2)^9} \quad (\text{C12})$$

Appendix D: Details of 2 + 1 Horn Calculation

1. $E_0^{\text{div}}(s)$

Renormalization of Brane Tension: We see in equation (35) that a pole remains^[15], specifically one that is z_b -dependent:

$$-\frac{9}{256} e^{-z_b} \times \frac{1}{s} \quad (\text{D1})$$

The Casimir force cannot be infinite, so clearly we must identify a physical parameter to absorb this divergence. Notice that this term is proportional to the volume of the brane

$$V_{\text{brane}} \propto \int_0^{2\pi} d\theta \sqrt{|\gamma|} = 2\pi e^{-z_b} = 2\pi e^{-z_b} \quad (\text{D2})$$

This suggests that the brane tension is a renormalizable quantity that will suffice. Let us consider the energy due to a bare brane tension, σ :

$$E_{\text{ten}} = \int_0^{2\pi} d\theta \sqrt{|\gamma|} \sigma = 2\pi e^{-z_b} \times \sigma \quad (\text{D3})$$

For convenience we define the renormalized brane tension using not only terms from E_0^{div} , but also the finite contributions to E_0 which are proportional to the brane volume (in the limit $z_b \rightarrow -\infty$):

$$E_{\text{ten}} \equiv 2\pi e^{-z_b} \sigma_{\text{ren}} \equiv 2\pi e^{-z_b} \left(\sigma - \frac{1}{2\pi} \frac{9}{128} \left(-\frac{13}{9} + \gamma + \frac{1}{2s} + \text{finite} \right) \right) \quad (\text{D4})$$

[15] See also Appendix E for an independent check using the heat kernel technique.

With this definition,

$$\lim_{z_b \rightarrow -\infty} E(z_b) \sim E_{\text{ten}} = 2\pi e^{-z_b} \times \sigma_{\text{ren}}, \quad (\text{D5})$$

which is now finite and independent of μ .

2. E_0^{rem}

From (36) we have

$$E_0^{\text{rem}} = \sum_{n=1}^{\infty} \left[-\frac{1 + 16x_b^2 + 49x_b^4 + 64x_b^6}{4(1 + 4x_b^2)^{5/2}} + \left(\frac{1}{2}x_b + \frac{9}{128}x_b^{-1} \right) \right] \quad (\text{D6})$$

and remind the reader that $x_b = |n|e^{z_b}$.

Limit $z_b \rightarrow \infty$: Since $x_b \gg 1$ for all n , we can expand in x_b^{-1} so that

$$\lim_{z_b \rightarrow \infty} E_0^{\text{rem}} \sim -\sum_{n=1}^{\infty} \frac{23}{1024} x_b^{-3} = -\frac{23}{1024} \zeta(3) e^{-3z_b} \quad (\text{D7})$$

Limit $z_b \rightarrow -\infty$: We can approximate the sum as an integral by using the Euler-Maclaurin formula which, to lowest order, says (see e.g. [26])

$$\sum_{n=1}^{\infty} f(An) \approx \frac{1}{A} \int_A^{\infty} dx f(x) + \frac{1}{2} (f(A) + f(\infty)) \quad (\text{D8})$$

We identify $A \leftrightarrow e^{z_b}$ so that $f(x_b)$ is the summand of (D6), thus

$$\begin{aligned} \lim_{z_b \rightarrow -\infty} E_0^{\text{rem}} &\sim e^{-z_b} \int_{e^{z_b}}^{\infty} dx f(x) + \frac{1}{2} f(e^{z_b}) \\ &\sim -\frac{7 + 18 \ln [4e^{z_b}]}{256} e^{-z_b} + \frac{1}{8} + \mathcal{O}(e^{2z_b}) \end{aligned} \quad (\text{D9})$$

3. E_0^{fin}

From (38) we have

$$E_0^{\text{fin}} = \frac{1}{\pi} \sum_{n=1}^{\infty} \int_{1/2}^{\infty} dk \frac{k}{(k^2 - \frac{1}{4})^{1/2}} D_k(x_b) \quad (\text{D10})$$

where

$$D_k(x_b) = \left(\ln [K_k(x_b) I_k(x_b)] - \tilde{\ln} [K_k(x_b) I_k(x_b)] \right) \quad (\text{D11})$$

Limit $z_b \rightarrow \infty$: Again, it will always be true that $x_b \gg 1$. Under this condition, the uniform asymptotic expansions for the modified Bessel functions are a good approximation because beyond the leading logarithmic term they are expansions in inverse powers of x_b . Therefore by going to the next highest order in x_b^{-1} we find (see Appendix C)

$$D_k(x_b) \approx \frac{(13x_b^6 - 232k^2x_b^4 + 288k^4x_b^2 - 32k^6)x_b^2}{64(x_b^2 + k^2)^6} \quad (\text{D12})$$

This can be directly integrated and, after performing another expansion in x_b^{-1}

$$\begin{aligned} E_0^{\text{fin}} &\approx \sum_{n=1}^{\infty} \frac{37\pi}{16384} x_b^{-3} \\ &= -\frac{37\pi}{32768} \zeta(3) e^{-3z_b} \end{aligned} \quad (\text{D13})$$

Limit $z_b \rightarrow -\infty$: Once again, we will use the lowest order Euler-Maclaurin expansion. In this limit one may show that

$$\lim_{x \rightarrow 0} D_k(x) \sim \mathcal{O}(x^2, x^{2k}) \quad (\text{D14})$$

depending on whether k is less than or greater than 1. This implies that to good approximation

$$E_0^{\text{fin}} \approx \frac{e^{-z_b}}{\pi} \int_{1/2}^{\infty} dk \frac{k}{(k^2 - \frac{1}{4})^{1/2}} \int_0^{\infty} dx D_k(x). \quad (\text{D15})$$

In the above expression we have lowered the lower limit of integration to zero, the error being roughly

$$e^{-z_b} \int_0^{e^{z_b}} dx D_k(x) \sim e^{-z_b} \int_0^{e^{z_b}} dx \mathcal{O}(x^2, x^{2k}) \sim \mathcal{O}(e^{2z_b}, e^{2kz_b}) \quad (\text{D16})$$

which is negligible as $z_b \rightarrow -\infty$. We have thus learned that in this limit $E_0^{\text{fin}} \propto e^{-z_b}$, so it remains to calculate this proportionality factor. Numerically computing the double integral in (D15), we find

$$E_0^{\text{fin}} \approx 2.4 \times 10^{-3} \times e^{-z_b} \quad (\text{D17})$$

Appendix E: Heat Kernel Analysis

The zeta function is intimately related to the heat equation (see e.g. [27]) as it is simply a Mellin transform of the heat operator. In this appendix we give a brief review of the heat kernel technique and apply it to confirm the poles encountered in $D = 2 + 1$, providing a partial check on our calculations.

1. Heat Kernel Analysis of a General $E_0(s)$

Following the nice review by Vassilevich [28] and book by Fursaev and Vassilevich [20], if we use a Mellin transform to write

$$\omega_{\mathbf{i}}^{1-2s} = \int_0^\infty dt \frac{t^{s-3/2}}{\Gamma(s - \frac{1}{2})} e^{-t\omega_{\mathbf{i}}^2} \quad (\text{E1})$$

then the zeta-function regularized Casimir energy (4) can be recast as

$$\begin{aligned} E_0(s) &= \frac{\mu^{2s}}{2} \sum_{\mathbf{i}} \omega_{\mathbf{i}}^{1-2s} \\ &= \frac{\mu^{2s}}{2} \int_0^\infty dt \frac{t^{s-3/2}}{\Gamma(s - \frac{1}{2})} K(t) \end{aligned} \quad (\text{E2})$$

where $K(t)$ is the heat kernel trace, given by^[16]

$$K(t) = \sum_i e^{-t\omega_i^2} = \sum_{p=0} t^{\frac{p-n}{2}} a_p \quad (\text{E3})$$

where n is the number of spatial dimensions and the heat kernel coefficients, a_p , are determined by integrals over local geometric scalars and also depend on the field type and boundary conditions. Considering (E3), in the limit $s \rightarrow 0$ the divergent terms of (E2) are those in which $p \leq n + 1$. Analytically continuing $s \rightarrow 0$ gives a finite answer for all terms except when $p = n + 1$; this is an inescapable pole. The divergence comes from the $t \rightarrow 0$ part of the integral, so we break the integral (E2) up into two regions, $[0, 1]$ and $[1, \infty)$. The

[16] Technically the summand should be $e^{-t\lambda_i}$, where the λ_i are the eigenvalues of the generalized Laplace-Beltrami operator. Since we use a simple massless Klein-Gordon field, $\omega_i^2 = \lambda_i$.

later converges, while the former contains the pole:

$$\begin{aligned} \frac{\mu^{2s}}{2} \int_0^1 dt \frac{t^{s-1}}{\Gamma(s - \frac{1}{2})} a_{n+1} &= - \frac{\mu^{2s}}{4\sqrt{\pi}} a_{n+1} \frac{t^s}{s} \Big|_0^1 + \mathcal{O}(s^0) \\ &\sim - \frac{1}{4\sqrt{\pi}} a_{n+1} \frac{1}{s} \end{aligned} \quad (\text{E4})$$

2. Heat Kernel Technique Applied to the $D = 2 + 1$ Geometries

To verify the poles in the Casimir energy encountered for both the horn and cone geometries in $D = 2 + 1$ ($n = 2$) we require the coefficient a_3 , for which we borrow the results from [28], suited for our problem and conventions. To apply them, we identify the variables from that work, (f, E, S, Π_+, Π_-) as $f = 1$, $E = 0$, and $S = 0$, with Π_+ and Π_- depending on the choice of boundary condition. With these results in hand, we have

$$a_3 = \frac{1}{768\sqrt{\pi}} \int_{\partial\mathcal{M}} d^{n-1}x \sqrt{|\gamma|} (16\chi R - 8R_{anan} + (13\Pi_+ - 7\Pi_-) K^2 + (2\Pi_+ + 10\Pi_-) K_{ab}K_{ab}) \quad (\text{E5})$$

where $\gamma_{\mu\nu}$ is the induced metric on the boundary, $\chi = \Pi_+ - \Pi_-$, the Riemann tensor is defined^[17] by $[\nabla_\mu, \nabla_\nu] A^\alpha \equiv R^\alpha_{\lambda\mu\nu} A^\lambda$, and K_{ab} is the extrinsic curvature tensor of the brane. Latin (or hatted) indices designate orthonormal coordinates, and repeated indices imply a summation. As we have split up both of the geometries into two regions, we take care to calculate a_3 on each side of the boundary separately, however, the answers are identical in the cases we consider.

a. Hyperbolic Horn

Here the determinant of the induced metric on the brane is given by $|\gamma| = e^{-2z_b}$, where we have set the horn curvature scale, $z_\star \equiv 1$. The relevant geometric objects are

$$R = -2 \quad (\text{E6})$$

$$R_{\hat{\theta}\hat{z}\hat{\theta}\hat{z}} = -1 \quad (\text{E7})$$

$$K_{ab} = \pm \delta_{a\hat{\theta}} \delta_{b\hat{\theta}} \quad (\text{E8})$$

[17] There is a difference of a minus sign between the Riemann tensor as defined in [28] and here.

where the sign of K_{ab} is positive (negative) if the normal to the boundary, n^μ points in the positive (negative) z direction.

Dirichlet Condition

Here we identify $\Pi_+ = 0, \Pi_- = 1$. For either region we find

$$a_3 = \frac{9}{128} \sqrt{\pi} e^{-z_b} \quad (\text{E9})$$

Considering (E4), we confirm that the entire pole part of the energy is

$$E_0^{\text{P}}(s) = -\frac{9}{256} e^{-z_b} \frac{1}{s} \quad (\text{E10})$$

Neumann Condition

Here $\Pi_+ = 1, \Pi_- = 0$. For either region we find

$$a_3 = -\frac{3}{128} \sqrt{\pi} e^{-z_b} \quad (\text{E11})$$

implying

$$E_0^{\text{P}}(s) = \frac{3}{256} e^{-z_b} \frac{1}{s} \quad (\text{E12})$$

b. Euclidean Cone

Here, the determinant of the induced metric on the brane is given by $|\gamma| = r_b^2$. As the geometry is Euclidean, only the extrinsic curvature tensor is non-zero:

$$K_{ab} = \pm \frac{1}{r_b} \delta_{a\theta} \delta_{b\theta} \quad (\text{E13})$$

where the sign of K_{ab} is positive (negative) if the normal to the boundary, n^μ points in the positive (negative) r direction.

Dirichlet Condition

Here $\Pi_+ = 0, \Pi_- = 1$. For either region we find

$$a_3 = \frac{(1 - \delta) \sqrt{\pi}}{128r_b} \quad (\text{E14})$$

Considering (E4), we confirm the entire pole part of the energy is

$$E_0^{\text{P}}(s) = -\frac{(1 - \delta) 1}{256r_b s} \quad (\text{E15})$$

Neumann Condition

Here $\Pi_+ = 1, \Pi_- = 0$. For either region we find

$$a_3 = \frac{5(1 - \delta) \sqrt{\pi}}{128r_b} \quad (\text{E16})$$

implying

$$E_0^{\text{P}}(s) = -\frac{5(1 - \delta) 1}{256r_b s} \quad (\text{E17})$$

